Recovery of Fe(III) from acid mine drainage and its subsequent application for the production of ferric chloride for drinking water coagulation

by

Mamile Belina Mahlohla

submitted in accordance with the requirements for
the degree of

MASTER OF SCIENCE

in the subject

Environmental Sciences

at the

UNIVERSITY OF SOUTH AFRICA

SUPERVISORS:

Prof Vhahangwele Masindi & Prof Memory Tekere

DATE

2024

DECLARATIONS

Name

Mamile Belina Mahlohla

Student number

20237871

Degree

Master of Science in Environmental Science

Recovery of Fe(III) from acid mine drainage and its subsequent application for the production of ferric chloride for drinking water coagulation

- I, Mamile Belina Mahlohla, affirm that the dissertation is solely my own creation. Furthermore, I have provided comprehensive references to acknowledge and indicate all the sources I have utilized or quoted.

- I further declare that I submitted the dissertation to originality checking software and that it falls within the accepted requirements for originality as stipulated in the ethics and legal frameworks of the University of South Africa.

- I declare that the above dissertation is solely submitted to the University of South Africa for the Master Degree of Environmental Sciences.

ACKNOWLEDGEMENTS

Firstly, I would like to thank God Almighty for being with me throughout this journey, for giving me strength, courage, and protection to complete this qualification. His everlasting love got me through it.

Secondly, I would also like to express my most heartfelt gratitude to my supervisors Prof Vhahangwele Masindi and Prof Memory Tekere for their support, willingness to impart valued knowledge and constant motivation in carrying out this research. I am truly grateful for your inputs, patience, and guidance. Your expertise, understanding, mentorship and experience made it possible for me to navigate and complete this challenging yet exciting journey.

I would also like to express my undiscounted appreciation to the following institutions and entities for their indispensable support through-out my project:

- University of South Africa (UNISA)
- Magalies Water (MW)
- Council for Scientific and Industrial Research (CSIR)
- University of Pretoria
- ROC Water Technology
- Mining houses and their management.
- Municipalities and their management.

These organisations, institutions and entities played a notable role in supporting the terminal objectives of this project. I am deeply indebted.

Finally, and most importantly, I would also like to thank my family, my partner, and my daughter Keitumetse Lesego Mahlohla for their prayers, support and always pushing me to be the best version of myself amid this challenging yet exciting journey.

DEDICATIONS

I would like to dedicate this MSc thesis to my daughter Keitumetse Lesego Mahlohla. She means the world to me, and I thank God for blessing me with her. She pushes me to be a better version of myself. I love her unconditionally. This MSc should serve as a sign of inspiration and source of possibilities to her.

ABSTRACT

Acid mine drainage (AMD) is a highly acidic and biorecalcitrant wastewater matrix that is rich in dissolved metals and wreaks havoc into receiving environments due to its toxic nature that poses mutagenic, teratogenic, and carcinogenic effects to living organisms on exposure. This is mainly triggered by embodied chemical species and their severe toxicological effects. Stringent regulatory frameworks require acid mine drainage to be contained and treated before it could be discharged to the receiving biosphere. In recent decades, there has been a shift in paradigm, where chemical species enshrined in wastewater streams present a different avenue of resource mining and could be recovered for beneficiation, especially when pragmatically and technically viewed under circular economy, waste beneficiation, and waste valorisation concepts. This study seeks to pursue such a quest as inspired by waste beneficiation and valorisation. Specifically, acid mine drainage is rich in Fe and sulphate contents due to the weathering of pyrite because of the parent mineral. The high iron (Fe(III)), i.e., post oxidation, content in AMD presents an opportunity for recovery and use for iron salt production hence the gross focus of this novel study.

This study focused on selective and fractional recovery of Fe(III) from real coal mine AMD, using magnesium oxide nanoparticles (MgO-NPs), and subsequently employ it for green production of ferric chloride ($FeCl_3$), a typical coagulant used in water and wastewater treatment. The goals of this innovative study were achieved by using a batch experimental method and protocol to optimize the conditions that are favourable for the removal of pollutants from rivers and wastewater. Specifically, the one-factor-at-a-time (OFAAT) were duly enacted, and they comprise the effect of contact time (mins.), effect of dosage (mL), and effect of mixing speed (rpm). Real water samples collected from the river was used for optimisation purposes. The quality of raw and final water was analysed in the SANAS/IEC/ISO 17025 accredited laboratory using state-of-the-art facilities such as photo spectrometers, ICP-MS, ICP-OES, Gallery plus discreet, and multi-parameter devises. Standard methods were also used to draw other technical conclusions. The composition of the recovered sludge from real AMD was characterised using X-ray fluorescence (XRF). Experiments were performed in triplicate and results were reported as mean values, with the cognizant of SDV of ≤ 5 for quality, repeatability, and trustworthiness of the obtained results. The efficacy of the synthetized ferric chloride was compared with the performance of commercial ferric chloride. Furthermore, its robustness and up-scalability were assessed using river water and municipal wastewater.

From the obtained results, optimum conditions were observed to be 0.2 mL/L (v/v ratio), 100 rpm of mixing speed, and 5 min of equilibration time. Under those conditions, the percentage removal efficacies for contaminants registered the following sequence: 99.8 ≥ 99.8 ≥ 99.7 ≥ 99.5 ≥ 99.2 ≥ 98.2 ≥ 95.3 ≥ 92.9 ≥ 81.1 ≥ 67.6 ≥ 52 ≥ 50 ≥ 48.8 ≥ 22.4 ≥ 11.8 ≥ 10.1 ≥ 10 ≥ 9.7 ≥ 6.7 ≥ 4.3% for Al ≥ ammonia ≥ turbidity ≥ Fe ≥ Cr ≥ Ni ≥ COD ≥ Mn ≥ Cu ≥ nitrite ≥ nitrate ≥ colour ≥ Ca ≥ alkalinity ≥ Mg ≥ K ≥ Na ≥ sulfate ≥ EC ≥ pH, respectively. Similar results were obtained when the same raw water was treated with commercially available $FeCl_3$, which is already used by the water and wastewater industry in South Africa. The results also highlighted that the AMD-synthesized $FeCl_3$ did not contain toxic heavy metals in its matrix, while the treated river water itself was within South African specifications for drinking water quality (SANS 241:2015). Interestingly, the efficacies of both the AMD-synthesized and commercially available $FeCl_3$ were assessed for water and wastewater treatment and were found comparable, and similar performance was observed with municipal wastewater. This highlights that AMD-synthesized $FeCl_3$ can be safely employed by the water and wastewater industry in South Africa and further afield and this will, although to a certain extent, address price and availability concerns surrounding commercial flocculants and coagulants. Furthermore, through AMD beneficiation, i.e., Fe(III) recovery, and partial acidity correction, water reclamation opportunities from AMD can be further pursued. Overall, resource recovery from waste and their reuse for treating other wastes can introduce sustainable paradigms and explicitly promote the United Nations (UN) sustainable development goals (SDGs). Future studies should look into pilot trials and mass production of ferric chloride using Fe(III) recovered from acid mine drainage, and this will ensure sustainability in the management of mine water and preserve the use of virgin materials for the production of ferric chloride.

Keywords:

Coagulation; flocculation; sustainable wastewater management; waste beneficiation and valorisation; resource recovery; acid rock drainage (ARD); acid mine drainage (AMD); municipal wastewater.

TABLE OF CONTENTS

LIST OF FIGURES AND TABLES

LIST OF FIGURES

LIST OF TABLES

ABBREVIATIONS AND ACRONYMS

Abbr.	**Meaning**	**Abbr.**	**Meaning**
AMD	Acid mine drainage	OFAT	One factor at a time
AQC	Analytical quality control	QA	Quality assurance
BET	Brunauer-Emmett-Teller	SDG	Sustainable Development Goals
FIB	Focussed Ion Beam	SEM	Scanned Electron Microscopy
HR	High Resolution	TGA	Thermo gravimetric analysis
REE	Rare earth elements	UN	United Nations
As	Arsenic	WHO	World Health Organisation
Cr	Chromium	SRB	Sulfate-reducing bioreactors
Cu	Copper	Al	Aluminium
Fe	Iron	Zn	Zinc
Ni	Nickel	HCl	Hydrochloric acid
Pb	Lead	Na	Sodium
Mn	Manganese		
Ca	Calcium		
NIST	National Institute of Standards and Technology		
SANAS	South African National Accreditation System		
FTIR	Fourier-Transform Infrared Spectrometer		
EDX	Energy-dispersive X-ray spectroscopy		
APHA	American Public Health Association		
ICP-MS	Inductively coupled plasma mass spectrometry		
ICP-OES	Inductively coupled plasma mass spectrometry		

NB: Please refer to the periodic table for chemical elements.

PUBLICATION OUTPUTS

Manuscripts

Mahlohla, MB., Masindi, V., Tekere, M., (2024). Recovery of Fe(III) from acid mine drainage and its subsequent application for the production of ferric chloride for water coagulation. Manuscript under review. Journal of Environmental Chemical Engineering _R1

Mahlohla, MB., Masindi, V., Tekere, M. 2024. A state-of-the-art review on the recovery of valuable minerals from acid mine drainage and their pragmatic beneficiation. Manuscript under review. Journal of Environmental Management.

Conference proceedings

Mahlohla, MB., Masindi, V., Tekere, M., (2024). Recovery of poly-cationic metal sulphate from acid mine drainage and its beneficiation as a coagulant for drinking water treatment. Accepted for oral presentation in the WVTF | IMWA 2024 conference. The WVTF – IMWA Congress 2024 · Morgantown, WV, USA 22 – 25 April 2024.

Patents

Mahlohla, MB., Masindi, V., Tekere, M. (2024). Novel method for the recovery of Fe(III) and its use to produce ferric chloride for water treatment. Provisional patent filed. Full patent filing in the Republic of South Africa (RSA) completed. The Patent Cooperation Treaty (PCT) patent under review in the World Intellectual Property Organization (WIPO).

CHAPTER ONE

INTRODUCTION

1.1 Background information

Consumerism along with rapid population growth, have put great stress on the demand for potable water in every part of the globe, hence posing a massive challenge to the water industry (Mavhungu et al., 2020a). The issue predominantly persists in Low- and Middle-Income Countries, including South Africa. Concurrently, the demand for virgin resources and feedstocks for water purification has proportionally increased and most of them are imported in South Africa, hence posing challenges particularly when viewed under the current supply chain disruption. As such, there is a need to come up with alternative sources and contingency plans for securing the chemicals that are used for water purification. This process is known for hefty chemical consumption. A typical water purification and treatment plant comprises screening, chemical dosing, sedimentation, filtration, and post chlorination. During chemical dosing, various chemicals are used, including polyelectrolytes (water-soluble organic polymers) and ferric compounds (ferric chloride or ferric sulfate) (Zafra et al., 2020). Until recently, polymers were the preferred option, however, after the 2022 Russian invasion of Ukraine, water utilities have resorted into the use of ferric salts as their alternative source of coagulant since monomers, which are the parent material of polymers, were not readily available due to Ukraine-/Russia-related sanctions and logistic challenges. Albeit, this problem was also extended, to a lesser extent, to ferric compounds as well, with the demand of iron coagulants being on the rise but their availability has decline on a global scale. A promising solution to this problem could be the beneficiation of the vast quantities of AMD that are excessively generated year-round in South Africa.

AMD from gold and coal mine comprises elevated concentrations of Fe, Al, Mn, and S, along with traces of other metals, which include heavy metals, rare earth metals, metalloids, radionuclides, oxyanions, and anions. The high concentration of Fe(III) and S in AMD makes it a suitable source for the harnessing of Fe species and this will then be employed towards the formation of Fe(III) species, including ferric sulfate ($Fe_2(SO_4)_3$) (Kefeni et al., 2017, Naidu et al., 2019, Chen et al., 2021). According to Brandt et al. (2017) Fe(III) salts have an excellent coagulating effect as they contain triple positive charges which neutralizes the negative charge on the colloidal particles. The authors also indicated that ferric chloride is more preferred than ferric sulphate as it performs better at very low doses. Numerous studies have explored the feasibility of producing sulphuric acid, gypsum, goethite, hematite, and magnetite from AMD (Simate and Ndlovu, 2014, Nleya et al., 2016, Kefeni et al., 2017). The recovery of goethite, hematite, and magnetite, as the Fe-based minerals, suggests the feasibility of recovering Fe(III) species from mine water which can be used for the treatment of drinking water (Masindi et al., 2015b, Akinwekomi et al., 2017, Akinwekomi et al., 2020).

In this regard, the utilization of authentic- AMD in aqueous form as a coagulant for drinking water purification has been suggested, but the presence of other heavy metals such as Zn suggested that the AMD needed pre-treatment before it can be used as a coagulant (Rao et al., 1992). Another study conducted by Menezes et al. (2009a) managed to produce poly-alumina-iron sulphate from coal acid mine drainage by chemical precipitation, Fe(II) was converted to Fe(III) by aerating AMD for 24 hours at pH 2.5- 3. The recovery and application were a success; however, the authors did not demonstrate the potential toxicity of using poly-alumina-iron sulphate due to the precipitation of other metals, therefore, there is a need to fill this gap. Nonetheless, the use of Fe(III) species recovered from AMD as a coagulant for drinking water purification has not yet been examined. As such, this will be the first study, in design and execution, to explore the feasible application of Fe(III) recovered from AMD as a coagulant for the treatment of drinking water. Furthermore, potential toxicity implications, based on the SANS-241 specifications and WHO standards, will also be explored. Lastly, different alkaline generating agents such as lime, limestone, hydrated lime (Maree and Du Plessis, 1993, Du Plessis and Maree, 1994, Geldenhuys et al., 2003), periclase, magnesite, brucite (Bologo et al., 2012, Masindi et al., 2017a, Masindi et al., 2018c), soda ash and caustic soda (Akinwekomi et al., 2017, Akinwekomi et al., 2020) have been employed for the treatment of AMD and recovery of valuable minerals. However, these minerals have different drawbacks and advantages, compared to lime and other Ca-based minerals, which have the challenges of precipitating metals, sulphates, metalloids, and anions. The Na-based reagents, i.e., soda ash and caustic soda, have high solubility and precipitate sulphate as Fe-based minerals thus leading to the contamination of Fe(III) by sulphate (Masindi and Tekere, 2020).

To date, Mg-based minerals have proven to be effective for the recovery of Fe(III) from AMD.. The complexation of Mg and S could explain this to form MgSO4(aq) with very high solubility, leaving Fe(III) precipitating predominantly. However, the use of Ca-rich Mg-based minerals accelerates the formation of gypsum and the Fe(III) sludge with sulphate. Therefore, this study seeks to use a high-grade Mg mineral, i.e., brucite, for the recovery of Fe(III) sludge and its use towards the production of ferric solution. The sludge will also be rich in Al and Mg hence making it rich in poly-cations hence enhancing its efficacy (Masindi and Tekere, 2020). Previous studies have demonstrated the feasibility of Fe(III) recovery, but the use of the recovered mineral as ferric chloride coagulant has never been explored and this makes this study the first in design and execution.

1.2 Problem statement

. The ever-increasing population and industrialization have put a strain on the iron ore due to its high demand. This has caused a deterioration in the high-grade iron ore. Albeit, South Africa produces 21% of the world gold output (Stilwell et al., 2000) but at the expense of the environment. Specifically, the mining of gold and coal leads to the production of AMD has been reported to pose hefty and notorious ecological impacts during its mining and processing. Therefore, AMD occurs when pyrite is exposed during the mining process, sulphuric acid and dissolved iron are produced by the reaction of the exposed pyrite with air and water. AMD from gold and coal mines encompasses elevated concentrations of Fe and S, among other elements which instigate great harm to the receiving waterbodies and the environment. Fe forms red, orange, or yellow sediments that are evidence of contaminated waterway. Fe at high concentrations is harmful to living organism as it causes nausea, vomiting, drowsiness, tachypnoea, seizures, and coma. It has detrimental aesthetic and plumbing impacts. A slight iron excess may occur in some people. Young children and sensitive persons may experience chronic health consequences in the 10 to 20 mg/L range, as well as sporadic acute symptoms at the higher end of this range. The discharge of AMD effluent from both coal and gold mines has left the receiving waterbodies highly polluted. AMD corrodes infrastructure as it is acidic and contains heavy metals. It is one of few factors that is responsible for water quality degradation and kills aquatic life in affected waterbodies. AMD has since been the most environmental problem facing the mining industry (Akinwekomi et al., 2020).

Due to its ecological impacts, AMD has become the focus of research innovation to produce ways to treat, recycle and reuse it (Masindi et al., 2022b). The comforting prospect is that AMD provides a reservoir for minerals hence prompting its recovery. The beneficiation of AMD through the recovery of Fe(III) species can protect the environment from ecological effects associated with unprocessed AMD and minimize the use of virgin materials by water treatment entities. Attributable to the above mentioned, it is crucial to valorise Fe(III) from AMD by recovering it via sequential and selective recovery and use it as a coagulant for the treatment of potable water. This will reduce pressure on the use of virgin materials hence fostering the concept of circular economy. Fe(III) coagulants or ferric salts are preferred as alternative coagulant because they produce denser flocs with superior settling properties and work better at lower doses (Brandt et al., 2017). Fe(III) coagulant acts as odorant, oxidizing and reducing agent. There are several studies which cover the recovery of minerals including Fe(III) from AMD, however, the use of synthesized Fe(III) as a coagulant has never been done, thus making this the first study in design and execution. Rao et al. (1992) had suggested the use of AMD as a coagulant but the study had some drawbacks, especially introduction of contaminants into product water. Albeit, this study will be the first to explore the feasibility of recovering superlative Fe(III) species and its application as a coagulant for drinking water treatment.

1.3 Aim and specific objectives

1.3.1 Aim of the study

The overall aim of this study is to recover Fe(III) from acid mine drainage (AMD), synthesize it to its ferric form and subsequently use it as a coagulant for drinking water treatment.

1.3.2 Specific objectives

To fulfil the aim of this study, the following specific objectives were pursued:

- To evaluate the physicochemical properties of acid mine drainage from mine water and river water before and after treatment.
- To optimize conditions that are suitable for the recovery of Fe(III) from AMD using MgO i.e., periclase, as a seeding material and its characterization.
- To explore the efficacy of the Fe(III)-based coagulant on the removal of indicator contaminants in drinking water.
- To compare the performance of commercially available ferric compounds and the synthesized Fe(III)-based coagulant on the removal of contaminants, including its compliance to SANS 241 specifications.
- To determine whether the recovered ferric is capable of leaching toxicants into the treated aqueous solutions.

1.4 Significance of the study

Food security and water scarcity have been amongst the most significant humanity plights, particularly affecting low and middle income countries (LMICs) (Besada and Werner, 2015). This is exasperated by the rapid population growth, climate change, and dilapidated state of wastewater handing facilities in LMICs settings (Mavhungu et al., 2020a). For the safety and benefits of the public, many efforts have been cascaded towards the effective management of water resources, yet there is ample room for improvement. Furthermore, the reliance on dwindling and finite resources for water purification has been an emerging problem of concern (Qureshi, 2020, Masindi and Foteinis, 2021). For example, for water purification, polyelectrolytes and metals based polymers are typically used for the removal of turbidity, suspended solids, and other contaminants embodied therein (Zafra et al., 2020). However, the COVID-19 pandemic and the 2022 Russian invasion of Ukraine have imposed great restrictions on monomers/polymers imports from developed countries, leading to exorbitant increases in the price of such chemicals and of other feedstocks which are essential for water purification as well as increased consumer reluctance (Khudaykulova et al., 2022).

On the other hand, acid mine drainage (AMD) is a wastewater matrix that emanates mainly from mining activities and prevalently from coal and gold mining. It comprises elevated concentrations of Fe and S, the later in the form of sulphate (SO_4^{2-}), which induce great harm to the receiving waterbodies, but at the same time render AMD a promising source for the harnessing of these minerals (Masindi et al., 2018a, Masindi et al., 2022a). Currently, conventional water treatment plants rely on the use of commercially available Fe(III), i.e., ferric iron, and lime for the treatment of drinking water. The primary aim is to remove dissolved chemicals, suspended solids, and colloids (Zafra et al., 2020). However, the feasibility of recovering Fe(III) from AMD, via sequential recovery, and its subsequent use as a coagulant for drinking water treatment has never been explored. In this regard, Rao et al. (1992) explored the use of real aqueous AMD as a coagulant, but the precluding factors were secondary contamination from the different embodied chemical species in the matrix of AMD. AMD is contaminated with a lot of contaminants; selective precipitation will be used as a way to recover the Fe(III) to avoid cross contamination or co-precipitation with other metals.

To this end, this study will recover Fe(III) from AMD via sequential precipitation and will use it, for the first time, in drinking water treatment. This will go a long way in minimizing the use of virgin materials by the water treatment industry and at the same time curtailing environmental impacts posed by AMD to different receiving environments. Furthermore, the use of the recovered Fe(III) from AMD will improve the sustainability of the mining process and concomitantly reduce the use of virgin and dwindling natural resources. Finally, this study will address the sustainable development goals (SDGs) as coined by UN and particularly goal number 6, which deals with the availability and sustainable management of water and sanitation.

1.5 Structure of the thesis

This document comprises of five (5) chapters integrated together to form a thesis. The chapters are assembled in a way that they give information of specific component of the thesis, of which, chapter 1- 5 are detailed as follows:

Chapter One (1):

This chapter gives a brief background of AMD and drinking water treatment coagulants. The magnitude of polymers scarcity in South Africa. Beneficiation of Fe recovered from AMD into a coagulant for drinking water treatment. Also, it highlights the aims and objectives of the study, the problem that was investigated, and justification of the study, amongst other components.

Chapter Two (2):

This chapter delves deeper into the formation of AMD, its causes, its effects on the environment, and the remediation options that are accessible are all thoroughly explained. The types of coagulants used in water treatment and mineral recovery from AMD are also explored. Also, ways to beneficiate minerals that are recovered from AMD are also discussed in light of drinking water treatment and further afield.

Chapter Three (3):

This chapter discusses materials and methods to be considered in a quest to achieve the overall goals of this study. This entails an in-depth explanation of the sampling procedures, recovery of Fe(III) by selective precipitation and production of ferric solution using HCl and its application. Specifically, it explicitly covers the optimization studies, sludge characterization, water quality and quality control procedures. It will also cover the quality control procedures in a quest to grossly highlight the creditability, repeatability, and trustworthiness of the obtained results.

Chapter Four (4):

This chapter will give detailed analysis of the results and discussions in light of the outlined objectives. It will also cover the quality control procedures and how the study relates to the body of knowledge. Specifically, the in-depth discussion of the performance of the two ferric in the removal of turbidity including its role on pH and EC. Furthermore, results on the robustness of the synthesized ferric using real samples from different sources will also be reported.

Chapter Five (5):

Finally, this chapter provided concluding remarks on the findings of this study in relation to the outlined main and specific objectives of this study. Thenceforth, the identified research gaps are enumerated as recommendations for future research avenues and pursuit. This will then be used to guide future research in areas that were unveiled from the findings of this study. Subsequently, the references for the used scientific studies will be included as the last section of the thesis for reference purposes.

CHAPTER TWO

LITERATURE REVIEW

This in-depth literature review meticulously delves deeper into the formation of AMD, its causes, its effects on the environment, and the accessible remediation options, which are all thoroughly explained. The types of coagulants used in water treatment and mineral recovery from AMD was also explored. Also, ways to beneficiate minerals that are recovered from AMD was also discussed considering drinking water treatment and further afield.

2.1 Introduction

AMD is a wastewater effluent that develops from intricate oxidation interactions that take place in both active and inactive mines under ambient circumstances (Yuan et al., 2022) and is predominated by, along with other elements, iron, aluminum, manganese, and sulphate. Due to varying effects on the quality surface water and groundwater, water released from operating, abandoned, and/or reclaimed coal sites with significantly higher acidity continues to be a global concern (Acharya and Kharel, 2020). AMD contains heavy metal pollutants which has a major negative influence on the biological environment and human health due to its toxicity, tenacity and non-biodegradability(Li et al., 2022).

2.2 Compositions of acid mine drainage

AMD comprise variety of chemical species and this is governed by variety of the seams that associates with the mineral in quest. Specifically, AMD that emanates from coal mining varies with AMD that emanates from gold mining. Research indicated that in some areas, AMD from gold mine have high concentrations of constituents as compared to the AMD from coal mines and vice versa. This is mainly due to the geographical location, geochemical and mineralogical data of the mine. The main cause of heavy metal contamination is the gold mining sector, which continuously releases pollutants into the environment. High concentrations of hazardous metals like Cu, Pb, Zn, Cd, As, and Hg that have an adverse effect on the environment are commonly found in AMD from gold mines. To date, researchers have pursued research in AMD that emanates from both sources and have reported variable amounts of different chemical species, which are summarised below the composition of the heavy metals in AMD is illustrated in **Table 2.1**.

Table 2.1: Heavy metals, element concentration in mg/L

Element	**Concentration**	**Source Mines**	**Reference**
Al	10-545	Coal	(Seo et al., 2017), (Kefeni et al., 2017), (Bortnikova et al., 2020), (Zhu et al., 2022).
	50-2830	Gold	
Fe	53.3-17640	Coal	(Heviankova et al., 2014) (Seo et al., 2017), (Bortnikova et al., 2020).
	460-8600	Gold	
Mn	5.17-300	Coal	(Heviankova et al., 2014), (Amaral et al., 2018), (Bortnikova et al., 2020) (Akinwekomi et al., 2020)
	18-2575	Gold	
Zn	0.2-102	Coal	(Zhu et al., 2020), (Xia et al., 2023a, Xia et al., 2023b), (Masindi, 2017a), (Brewster et al., 2020) (Bortnikova et al., 2020)
	0.01-140	Gold	
Cu	0.05-320	Coal	, (Masindi et al., 2017b, Masindi, 2017c), (Brewster et al., 2020), (Vadapalli et al., 2008)
	0.01-65	Gold	
Cr	0.01-1.29	Coal	(Zhu et al., 2022), (Bortnikova et al., 2020)
	3.2-20	Gold	
Pb	0.12-58.3	Coal	(Masindi, 2017b, Masindi et al., 2017b), (Bortnikova et al., 2020)
	0.01-6.4	Gold	
Ni	1.1-922	Coal	(Vadapalli et al., 2008), (Wei et al., 2005), (Masindi, 2017b), (Cánovas et al., 2016)
	1.16-579	Gold	
Cd	0.001-1378	Coal	(Chen et al., 2021), (Bortnikova et al., 2020), (Cánovas et al., 2016)
	0.01-171	Gold	
Co	0.01-640	Coal	(Mwewa et al., 2019a, Mwewa et al., 2019b), (Sahoo et al., 2012) (Masindi et al., 2017b).
	0.01-41.3	Gold	

AMD occurs when sulfide minerals like pyrite oxidises. Acidity is produced when metal sulphides, (typically pyrite, which is iron sulfide) inside the surrounding rock and overburden oxidize after being exposed to air and water. Despite the fact that the processes also take place in an abiotic environment, colonies of bacteria and archaea significantly speed up the breakdown of metal ions. These microorganisms, known as extremophiles for their capacity to endure extreme circumstances, are found naturally in the rock and prefer acidic conditions of abandoned mines but their abundance is often constrained by availability of oxygen and water. Runoff and seepage from building materials, open pits mines, tailing, reserves and rock cuttings are the primary sources of AMD (Acharya and Kharel, 2020). The category and aggregate of sulfide minerals present determine the composition and concentrations of metals in AMD. The acid- and alkaline-producing (sulfide and carbonate) minerals found in the disrupted rock affect the drainage quality coming from underground excavation or backfills of surface mines. The composition of alkali and alkaline earth metals present in coal and gold AMD is illustrated in **Table 2.2.**

Table 2.2: Alkaline metals, element concentration in mg/L.

Element	Concentration	Source Mines	Reference
Na	0.1- 168	Coal	(Sahoo et al., 2012), (Masindi et al., 2018b), (Bortnikova et al., 2020)
	22-171	Gold	
K	0.01-28.3	Coal	(Sahoo et al., 2012), (Craw et al., 2023)
	1-18	Gold	
Ca	15.6-1070	Coal	(Seo et al., 2017), (Heviankova et al., 2014), (Amaral et al., 2018), (Sahoo et al., 2012)
	15-762	Gold	
Mg	7-474	Coal	(Zhu et al., 2020), (Xia et al., 2023a, Xia et al., 2023b), (Mwewa et al., 2019b).
	97-4564	Gold	
Alkalinity	0.06-14	Coal	(Masindi et al., 2017b) (Kirby and Cravotta, 2005), (Craw et al., 2023)
	16- 640	Gold	
Acidity	214-8133	Coal	(Sahoo et al., 2012), (Masindi et al., 2017a) (Cánovas et al., 2016).
	413-4200	Gold	

Gold and coal extraction creates enormous volumes of unprofitable sulfidic waste rock, which, if exposed to the atmosphere, is vulnerable to increased precipitation infiltration and weathering. The mining sector is a constant source of pollution, representing the main source of metalloids and oxyanions contamination during the mining process and for many years after the mining activity is terminated. Numerous redox-sensitive metals and metalloids can produce oxyanions. These species' toxicity, non-degradability, and movement in aquatic habitats make them dangerous to living things even at low concentration (Luptáková et al., 2019) . Sulphates are found in high concentrations in AMD from both coal and gold mines. Oxyanions, which behave quite differently from metals and metalloids, are formed when arsenic and selenium combine. Arsenic is a metalloid that occurs naturally and is significantly toxic. Different concentrations of metalloids and oxyanions from cold and coal acid mine drainage are illustrated in Table 2.3

Table 2.3: Metalloids and oxyanions, concentration in mg/L, except Eh in mV.

Elements	**Concentration**	**Source Mines**	**Reference**
As	0.02-32.2	Coal	Masindi et al (2017), (Bortnikova et al., 2020)
	0.02-1300	Gold	
B	0.01-1.1	Coal	(Vadapalli et al., 2008), (Craw et al., 2006), (Masindi et al., 2015a)
	0.01-5	Gold	
Si	0.01-30	Coal	(Masindi et al., 2015a), (Masindi et al., 2018c)
	0.01-1.5	Gold	
Sulphates	1950-30000	Coal	(Seo et al., 2017),(Masindi, 2017a) (Brewster et al., 2020)
	4000- 29547	Gold	
Oxidation-reduction potential	119-568	Coal	(Cheong et al., 2012) , (Zhao et al., 2007), (Bortnikova et al., 2020)
	10-657	Gold	

AMD comprise holmium, terbium, lanthanum, yttrium, europium, cerium, thulium, lutetium, praseodymium, ytterbium, neodymium, promethium, scandium, samarium, gadolinium, dysprosium, and erbium in its matrices primarily due to their co-weathering from embodying stratigraphy (Merten et al., 2005, Mwewa et al., 2022b). Rare earth elements, which are still highly important due to the rising demand for them as a result of their essential and indispensable application in many high-tech sectors today, can be found in AMD. AMD develops when pyritic waste rock from coal and gold mines is exposed to air. The rare earth elements (REE) are subsequently extracted from the rock by this acid. The REE can be extracted and processed into commercially viable products from the concentrated sludge left over after AMD treatment(Ziemkiewicz et al., 2021). **Table 2.4** illustrates the concentrations of REEs from different sources.

Table 2.4: Rare earth elements, concentration in μg/L.

Elements	Concentration	Source Mines	Reference
Lanthanum (La)	0.005-845	Coal	(Cravotta III, 2008), (Ma et al., 2018b), (Pereira et al., 2023)
	3.4-38.4	Gold	
Cerium (Ce)	0.01-5510	Coal	(Cravotta III, 2008), (Ma et al., 2018b), (Brewster et al., 2020)
	8.1-210.4	Gold	
Praseodymium (Pr)	2.78-148	Coal	(Sahoo et al., 2012), (Zhao et al., 2007), (Goodman et al., 2023)
	0.9-56.7	Gold	
Neodymium (Nd)	0.001-310	Coal	(Cravotta III, 2008), (Ma et al., 2018b), (Brewster et al., 2020), (Goodman et al., 2023).
	3.7-222.5	Gold	
Samarium (Sm)	0.005-154	Coal	(Cravotta III, 2008),(Brewster et al., 2020), (Zhao et al., 2007)
	1.1-72	Gold	
Europium (Eu)	0.87-37.1	Coal	(Sahoo et al., 2012), (Zhao et al., 2007) (Pereira et al., 2023), (Goodman et al., 2023)
	0.3-10.2	Gold	
Gadolinium (Gd)	0.008-168	Coal	(Zhao et al., 2007, Brewster et al., 2020)
	1.4-81	Gold	
Terbium (Tb)	0.70-28.5	Coal	(Zhao et al., 2007), (Goodman et al., 2023)
	0.2-7.1	Gold	
Dysprosium (Dy)	0.002-132	Coal	(Zhao et al., 2007, Brewster et al., 2020)
	1.5-77	Gold	
Holmium (Ho)	0.87-35.5	Coal	(Zhao et al., 2007), (Ma et al., 2018a, Ma et al., 2018b), (Sahoo et al., 2012)
	0.3-7.6	Gold	
Erbium (Er)	2.43-56.8	Coal	

	0.9-19.9	Gold	(Zhao et al., 2007), (Goodman et al., 2023)
Thulium (Tm)	0.34-12.3	Coal	(Zhao et al., 2007), (Sahoo et al., 2012), (Goodman et al., 2023)
	0.1-4.7	Gold	
Ytterbium (Yb)	1.99-51.2	Coal	(Brewster et al., 2020), (Zhao et al., 2007), (Sahoo et al., 2012)
	0.7-382	Gold	
Lutetium (Lu)	0.31-10.4	Coal	(Zhao et al., 2007), (Sahoo et al., 2012), (Goodman et al., 2023)
	0.1-4.0	Gold	
Scandium (Sc)	1.0-112	Coal	(Cravotta III, 2008, Ma et al., 2018b)
	0.6-27	Gold	
Yttrium (Y)	0.11-2050	Coal	(Ma et al., 2018b), (Cravotta III, 2008)
	8.6-18	Gold	

Radionuclides often occur naturally in soil or in water in concentrations that are not potentially hazardous to human health (Kamunda et al., 2016) but human activities such as mining often results in radionuclides being exposed to the environment. When the levels rise as a result of human activities like mining or natural disasters like earthquakes, it is quite concerning. It is understood that radionuclides are usually an issue of concern when uranium ore is mined (Fernandes et al., 1998). Conversely, traces of radionuclides have been found in coal and gold mining which results in their concentration being elevated to harmful levels. AMD has already been shown to have the ability to mobilize large amounts of radionuclides and introduce them into the environment. These radionuclides whether inhaled in dust or consumed in water, may produce ionizing radiation which is harmful to the cells and tissues in the body as they are carcinogenic. The composition of radionuclides in gold and cold AMD is illustrated in **Table 2.5.**

Table 2.5: Radionuclides, concentration in Bq/L except uranium coal in mg/L.

Elements	Concentration	Source Mines	Reference
Uranium (U)	0.2-765	Coal	(Galhardi et al., 2017), (Kamunda et al., 2016), (Goodman et al., 2023), Masindi (2018)
	0.29-2668.9	Gold	
Thorium (Th)	0.1-11.9	Coal	(Smołka-Danielowska and Walencik-Łata, 2021, Goodman et al., 2023), (Kamunda et al., 2016),
	0.7-80.7	Gold	
Radium (Ra)	0.002-49.70	Coal	(Wysocka et al., 2019), (Kamunda et al., 2016)
	76-2811,9	Gold	
Radon (Rn)	0.43-44.7	Coal	(Galhardi et al., 2017), (Moshupya et al., 2019)
	32- 1060	Gold	

AMD is notorious for its environmental pollution, and it contains elevated concentrations of heavy and toxic elements. The above-mentioned elements can be toxic to human health at elevated concentrations, and they can also result in numerous eco-toxicological effects. AMD is still regarded as the biggest sustainability concern in mining because of the enormous amounts of waste that are produced and the expensive related treatment costs. The paradigm is shifting towards sustainable development which focuses on recovering valuable minerals from AMD at low cost. This opens avenue and foster the concept of circular economy. The researchers are developing initiatives to address the problems associated with AMD, recovery of minerals being the forefront of the initiatives. AMD is a secondary source for mineral recovery and the concentration of elements in AMD determines their recoverability. Some elements are available in minutes concentration, and they are not recoverable hence impairing their economic and commercial values. Those that are recoverable could be recovered and used in the industries. As a result, less virgin material will be used and opportunities for beneficiation and valorisation will arise (Anyakora et al., 2012).

2.3 Recovery of valuable minerals from acid mine drainage

2.3.1 Recovery of Al, Fe, Mn, Cu and Zn

AMD contains significant concentration of dissolved precious metal ions such as Fe, Mn, Pb, Cu, Zn, Al, (Masindi et al., 2022b), which could be hazardous to human health and the nearby environment. Resolving possible pollution problems can be achieved with the recovery and reuse of these valuable resources. The recovery of these valuable metal ions has steadily been the focus of the study in recent years, shifting gradually from prevention and treatment of AMD. In light of that, AMD is predominated by Fe and S as major contaminants and intermediates of Al and Mn, followed by traces of other metals. Traditional lime neutralisation and biological treatment procedures are being used to treat AMD with elevated iron concentrations (Hu et al., 2022). Rao et al. (1992) studied acid mine drainage as a coagulant. The main quest was to examine a 3-step selective precipitation technique of recovering Fe as iron hydroxide ($Fe(OH)_3$). Lime was added at constant mixing until the pH was 3.5-3.6. The separation of $Fe(OH)_3$ was achieved by filtration from the solution. Hu et al. (2022) reported the use of NaOH for the recovery of Fe(III) from aqueous solution. The study demonstrated and confirmed the feasibility of recovering Fe(III) from AMD and explore its potential beneficiation. The experimental results indicated 99.43% iron removal rate. Akinwekomi et al. (2020) demonstrated the recovery of Fe sludge through selective precipitation, which was accomplished by gradually increasing the pH from 2 to 4.5 by adding 0.5 ml of a 10% sodium carbonate solution. After settling, the supernatant was filtered to recover the valuable minerals. This process does not need sophisticated technologies to oxidise Fe(II) to Fe(III). Furthermore, Masindi et al. (2018c) evaluated the combination of experimental and geochemical modelling studies using calcined cryptocrystalline magnesite nano-sheet to illustrate the fractional and step by step recovery of minerals from AMD. In their study, the authors demonstrated the recovery of Fe(III) at pH <3.5 in addition to other minerals such as calcium sulphate (gypsum)≥4-9, Al≥4-6.5, Mn≥8-9.5, Cu≥6-7, Zn≥6-8, Pb≥6.5-8, and Ni≥9.5. Albeit, the wide precipitation range of sulphate hinders the recovery of pure minerals unless Ca free Mg or Na minerals are used as seeding materials for the precipitation of metals. Flores et al. (2012) recovered iron oxides from AMD using a sequential precipitation method. The authors neutralized AMD by addition of $\mathrm{Ca(OH)_2}$ to increase the pH to 3.8, after that calcium sulfate and aluminium hydroxide settled. $\mathrm{Fe(OH)_2}$ was precipitated with neutralization by adding NaOH which was followed by slow oxidation of $\mathrm{Fe(OH)_2}$. Thermal treatments were carried out at temperatures ranges from 100-700 °C. The results from this study indicate that AMD can be a source of raw material for iron oxide production. Silva et al. (2012b) evaluated the production of magnetite particles acquired from iron recovered from AMD by utilizing selective precipitation/ UV. Iron was recovered by selective precipitation of AMD at pH 3.6. The same technique was previously used by Wei et al. (2005) and Menezes et al. (2009a). Iron was precipitated as ferric hydroxide by adding 4 N NaOH in the solution to increase and maintain pH of AMD at 3.6 ± 0.1. Separation was done by centrifugation at 3000 rpm. In order to create an iron solution for magnetite solution, the final precipitate was dissolved in sulphuric acid 5 mL and diluted in 1L of water. The final precipitate was dissolved with 5 mL sulphuric acid and diluted in 1 L of water to achieve an iron solution for magnetite production. On another study, Wei et al. (2005) recovered iron and aluminium by selective precipitation from AMD. High quality iron and aluminium hydroxide were recovered using a two-step selective precipitation, where >93.4% and >98.6% iron purity were recovered at pH 3.5-4.0 respectively. However, aluminium was recovered at pH 6.0-7.0 with recovery of > 97.2% and >92.1% respectively, using the AMD water after iron recovery. The results obtained from their study corroborate what has been reported in previous work (Seo et al., 2017). Le et al. (2020) recovered Al(III) and Fe(III) from AMD through sequential selective precipitation and fluidized bed homogeneous crystallization. The results obtained shows that Fe(III) precipitated at pH 3.0-4.0 as ferric hydroxide precipitates while Al(III) precipitated at pH 5.5-7.5 as aluminium hydroxide. The RBHC results indicated the recovery of Al(III) at pH 9.25 with up-flow velocity of 30.50m/h and molar ratio of $[H_2O_2]/[Al(III)]$. Removal efficiencies achieve was 99.8% for Fe(III) and 98.9% for Al(III). Furthermore, other metals like Mn have been recovered because of their composition in acid mine drainage. (Silva et al., 2012a) conducted a study to precipitate manganese from mine water. In their study, they used 0.67 g/L of Na_2CO_3 and 12.5 g/L of $CaCO_3$ which resulted in 99.9% removal efficiency at pH $\geq$ 8.5 and the excess manganese(II) concentration of 0.14 mg/L from initial concentration of 140 mg/L. (Yuan et al., 2000) explored the oxidation and recovery of manganese in a manganese ore leaching mixture by utilising chlorine salt ($NaClO_3$) as an oxidizing agent for manganese(II) in the acidic solution. The results showed that 90% of the manganese was recovered. Furthermore, Zn and Cu are also recoverable due to their available concentration in AMD. MacIngova and Luptakova (2012) recovered metals (Fe, Al, Cu, Mn, and Zn) from AMD by sequential selective precipitation (SSP) process. (Sahinkaya et al., 2009) investigated the separate precipitation of Cu and Zn from AMD using sulfide which was produced in an anaerobic baffled reactor (ABR). Using sulfide delivered from ABR effluent via N2 gas, Cu was precipitated independently at low pH 2, taking 45–60 minutes to complete, whereas Zn did not precipitate during Cu removal. The removal efficacy was >84%. Conversely, Zn was recovered after Cu precipitation using ABR effluent composed of alkalinity and sulfide. The removal efficacy of Zn was between 84% and 98%, depending on the volume of the ABR effluent mixture

. The above results authenticate what has been reported in literature.. (Pino et al., 2020) examined the feasibility of Cu recovery from real AMD through pilot-scale tests. Cu was concentrated from AMD solution through the use of nanofiltration which was subsequently extracted from the concentrated nanofiltration solution using solvent extraction. The initial concentration of Cu in AMD was 531,2 mg/L and the outcomes of this study demonstrated that nanofiltration combined with solvent extraction is favourable for Cu recovery, with the recovery efficacy of 97%. Oh et al. (2016) evaluated the recovery of Cu and Zn by selective precipitation from AMD on an active mine on a pilot-scale. The researchers demonstrated that the precipitation rate was strongly dependent on coagulant dosage and AMD flow rate. At 1.40 L/min AMD flow rate and 110.6 mg/L of Na_2S, 90% precipitation rate with 80% purity was observed. This study proves that selective precipitation can be carried out in a field and not only on a laboratory basis. Furthermore, Tabak et al. (2003) investigated the use of selective, sequential precipitation to recover metals as hydroxide and sulfides from AMD. The metal bio recovery and recycling method is in accordance with the complete separation of the biological sulfate reduction stage and the metal precipitation step. In the precipitation process, hydrogen sulfide generated in the SRB bioreactor systems is utilized to create insoluble metal sulfides. The SSP method recovered 99.8% of aluminium (as hydroxide), 99.7% of cadmium (as sulfide), 99.1% of cobalt (as sulfide), 99.8% of copper (as sulfide), 97.1% of manganese (as sulfide), 47.8% of nickel (as sulfide), and 100% of zinc (as sulfide). Ferric hydroxide ≥ zinc sulphide ≥ metals ≥ aluminium hydroxide ≥ copper sulphide ≥ manganese sulphide with the average precipitation purity of 97.5% ≥ 95.6% ≥ 92.4% ≥ 92.1% ≥ 81.5% ≥75.0%, respectively. The final produced water comprised just calcium and magnesium, and the quantities of sulfate and sulfide were both below potable water limits (Tabak et al., 2003). This agriculturally useable water reached the EPA's gold standard requirement for water quality. Although many technologies have been explored when it comes to recovery of metals from AMD by researchers, but the most preferred method is selective precipitation.

2.3.2 Recovery of rare earth elements

AMD is comprised of REEs, which are available at recoverable concentrations. Due to its vital indispensable application in many high-tech industries today, rare earth elements which are present in AMD, continues to be of great importance. An increase in production should be enough to meet the rising demand for REEs (Mwewa et al., 2022a). A study conducted by Chávez (2017) indicated that phosphate precipitation as a different method for recovering REEs from acid mine water. This is brought on by the lanthanides' and yttrium's stronger attraction for the phosphate conjugate than for the sulphate. It is anticipated that the precipitation of REEs as phosphates will begin when the phosphate ions are added to the REEs-containing solution. In particular, using residual of phosphate (P/REE (40)) REE recovery percentage of 90±5% were attained. Royer-Lavallée et al. (2020) removed and potentially recovered rare earth elements from mine water. Sorption and precipitation were discussed in detail as the main techniques for the removal of REEs from real and synthetic mine water. The results indicated that the initial REE present in the real AMD was between 3,6 and 200 µg/L and through the use of nZVI dosed at 4.0 g/L at optimum pH of 2,5-and 30-minutes contact time, >99.9% of REE have been removed from real AMD. On another study, it was demonstrated that Beltrami et al. (2015) recovered 95% of the REEs from a mixture containing 250 mg/L of REEs and elevated concentration of iron (32, 300 mg/L) in a different investigation. From this work, it was shown that AMD, which is often treated as waste, can be recovered, and used to produce pure REEs that has myriads of industrial applications. (Felipe et al., 2021) conducted a study on the recovery of rare earth elements from AMD using ion exchange. In their work, the authors used cationic exchange resin to recover the REEs and the experiments were conducted at pH values 1.4, 2.4 and 3.4 with different resins. The results from this study demonstrate that at all pH values, the resins exhibit greater selectivity for light REE. This study indicated that the resins selected light REE than heavy REE (light REE > Heavy REE) and pH 1.4 and 3.4 were more favourable. On another study, (Hermassi et al., 2022b) recovered REE from AMD using a three-stage process to selectively separate REE from metals. Firstly, Fe (II) was oxidized to Fe(III) and followed by precipitation at pH 3,6 ± 0.2. Sulfonic ion-exchange resin was used to extract FEE from AMD and produce concentrated REE sulfuric solutions up to 0.25 gREE/L. Lastly, REE was selectively separated from metals through precipitation with phosphate solution under optimized pH. XRD analysis from this study identified Xenotime (YPO4(s)) and Cheralite (CePO4(s)) as the main minerals. (Moraes et al., 2020) investigated the co-precipitation of FEE and Fe and Al as primary co-precipitates from AMD utilising Al and Fe oxyhydroxides. AMD was neutralised with potassium hydroxide to produce an amorphous precipitate which contains 14% of REE oxides. At pH value 8, the Al13-polymer precipitate accounts for the removal of REE while concurrently enhancing adsorption and entrapment. This study demonstrated that 60% of REE could be leached via sequential extraction using acetic acid. This is followed by the co-precipitation of REE and uranium by Fe-Al precipitates in AMD. It was determined that the presence and quantity of Fe in the initial solution, particularly in acidic settings, can positively influence the REE removal efficacy. Due to the high demand for REEs, Vaziri Hassas et al. (2020) utilised a novel staged precipitation for the recovery of FEEs from AMD collected from both operating AMD treatment facility. Staged precipitation is considered environmentally friendly, efficient and it is cheaper than most technologies. The experiments were conducted using $\mathrm{CO_2}$ mineralization process and NaOH. The results from this study indicated ≥85% of REEs and ≥90% of Al were recovered through $\mathrm{CO_2}$ mineralization process at pH values below 7. Goodman et al. (2023) also explored the use of two-stage for the recovery of REEs from AMD. In the first stage, thorium was removed by adsorption while iron was precipitated. On the second stage aluminium was precipitated and REEs were removed by adsorption. The REEs were recovered at 90%. The results from the above studies demonstrate the feasibility of recovering FEEs from AMD successfully.

2.3.3 Recovery of sulphate

Sulphate is the most predominant element in AMD, and this is attributed to the oxidation of pyrite (FeS) in the lithologies that surround the coal seam or strata. This increases the viability of recovering sulphate from AMD as many minerals that have commercial values. Specifically, sulphate can be recovered as gypsum, sulphuric acid, and elemental sulphur, thus enabling its variety of application depending on the amenability of the application and process. Various studies have illustrated the recovery of sulphate from AMD, specifically, the study conducted by Akinwekomi et al. (2020) documented that the water treated is rich in sulphate which is recovered through the addition of lime to synthesize high grade gypsum (calcium sulphate). A study conducted by (Ntuli et al., 2016a), Ntuli et al. (2016b) illustrated the use of de-silicated fly ash (DFA) in order to remove sulphate from AMD. In this study, DFA was used as an adsorbent originating from fly-ash through leaching out silica. The parameters tested for the removal of sulphate were DFA amount, residence duration, and temperature. A 2% DFA addition removed more over 50% of the sulphate. More contact is allowed on DFA as the time is extended, and a clear rise in sulphate removal is noted. The temperatures tested were 25, 35, and 45 °C. At temperatures and residence duration of 35 °C and 90 minutes, respectively, a 2% DFA solid loading resulted in the greatest sulphate removal of 75%. DFA's maximal adsorption capacity was determined to be 147.06 mg/g DFA. The Langmuir isotherm and pseudo second order kinetics governed the sorption mechanism. The results from this study demonstrated that DFA is more attractive alternative adsorbent for the removal of sulphate from AMD. Sulphate is available in high concentrations in AMD which makes it economically recoverable. Pratinthong et al. (2021) conducted a study on the removal of sulfate from lignite coal mine drainage in Thailand. Ettringite precipitation was used to investigate the ideal conditions utilizing Central Composite Design. On the sulfate removal efficiency, the impacts of Ca/S and Al/S ratios, reaction time, and temperature were examined. The statistical analysis revealed that the Al/S ratio and reaction time had a substantial effect on the efficiency of sulfate removal. When the Al/S ratio and reaction time are raised, the efficiency of sulfate removal increases. The anticipated reaction yielded an ideal reaction time of 6.14 h, meanwhile the Ca/S and Al/S ratios were fixed at 4 and 4.5, respectively, at room temperature. Under these conditions, the percentage removal efficiency was 99.6% and 99.0%, respectively. The XRD results correspond with most of the precipitation results at room temperature. Furthermore, an increase in temperature led to the formation of monosulfate, specifically at 80 °C. On the other hand, researchers have investigated different techniques to recover sulphate from AMD, among them is membrane filtration. Membrane filtration have been studied due to its ability to remove contaminants from water and reclaim drinking water (Mavhungu et al., 2020b). (Agboola et al., 2017) investigated the use of nanofiltration for ion separation from AMD employing two composite nanofiltration membranes (Nano-Pro-3012 and NF90) as examples of acid-stable polyamide membranes. Because the fouling effect is feasible at lower pH levels, greater cation removal was seen in both membranes at higher pH values. In contrast, the study found that anions were removed more effectively at lower pH levels. Finding the right operational pH value trade-off is so critical. When compared to the Nano-Pro-3012 membrane, the rougher NF90 membrane removed more sulphate. The examined water sample contained 3500 mg/L of sulphate, and the sulphate removals were 97.6% and 86.3%, respectively, for NF90 and Nano-Pro-3012 at pH 2.2. Furthermore, (PreuB et al., 2012b), PreuB et al. (2012a)evaluated the performance of nanofiltration membranes for sulphate removal from mine drainage. The experiments were conducted on mine water treated with lime. The concentration of the sulphate before nanofiltration was recorded as 1850 mg/L and 65 mg/L after nanofiltration treatment. The removal efficiency was 96%. The removal of sulphate was investigated by Nogueira et al. (2021) using sugarcane vinasse as electron donor to remove sulphate from synthetic AMD. The authors applied the down flow structured bed bioreactor (DFSBR) to reduce sulphate. The DFSBR was operated at different phases, at pH values between 6.7-7.3 and the removal efficiencies were recorded to be between 55% and 91%. The 55% removal efficacy was obtained at pH 6.8 and 91% was obtained at pH 7.3, respectively. On the other hand, sulphate can be recovered as sulphuric acid. This was demonstrated in the study conducted by Martí-Calatayud et al. (2014) where sulphuric acid was recovered from AMD using three-compartment electrodialysis (ED). The co-ion exclusion mechanism in the membranes resulted in an excellent recovery of sulfuric acid free of Fe(III) species in the anode compartment. The difference in pH and pSO_4^{2-} levels between the membrane phase and the external electrolyte promotes complicated species dissociation within the membranes. This phenomenon impedes the passage of complex ions of Fe(III) and sulphates toward the anodic and cathodic compartments, respectively. The anion-exchange membrane's current efficiency ratings at varying current densities were nearly stable over time. However, when the current increases, the increase in acid recovery decreases. This result is explained by a shift in the equilibrium at the membrane/solution interface as more SO_4^{2-} cross the anionic membrane, as well as an increase in water dissociation when the limiting current density is exceeded. The fundamental restriction of the technique is an abrupt increase in cell voltage caused by precipitates forming on the surface of the cation-exchange membrane. Kesieme et al. (2012) recovered sulfuric acid from AMD generated by mining operations using the direct contact membrane distillation (DCMD) technique. The experimental results revealed that when the temperature of the feed solution was kept at 60 °C and the flux was kept between 20 and 31 kg/m2/h, the sulfate separation efficiency could reach more than 99.9% removal efficacy. On another study conducted by Nleya et al. (2016) Dowex MSA-1 ion exchange resins were used to test sulphuric acid recovery from metal barren solution. The results demonstrated that sulphuric acid may be recovered by the resins using the acid retardation process and then upgraded to near market values of up to 70% sulphuric acid using an evaporator. Mulopo (2016) investigated the conversion of $CaSO_4/Mg(OH)_2$ and $BaSO_4/CaCO_3$ during AMD treatment with the aim to recover sulphur. Specifically, the thermal decomposition of gypsum and barite/calcite sludge to calcium sulphide and barium sulphide, respectively, were investigated. H_2S was stripped from barium sulphide and calcium sulphide slurry with CO_2 to form H_2S gas. The H_2S produced was treated with ferric sulphate to produce elemental sulphur. Sulphur with purity ranging between 95.2% and 99.1% was recovered from sulphate-rich wastes.

2.3.4 Drinking water reclamation

According to literature, approximately 360 ML of AMD is produced from both the coal and gold fields, specifically the western, central and eastern basin for gold mines, and Mpumalanga highlands for coal mines (Nleya et al., 2016). The volume of mine water produced in a day is gigantic and demonstrate an indispensable commercial or economic model. Amid that, South Africa is regarded as a water scarce country which is further exasperated by pressing issues of climate change drawing calamitous plight water resources, i.e., quantitatively, and qualitatively. Beneficiation of AMD is gaining momentum with opportunities for water reclamation which can be utilised for different purposes including drinking water, irrigation or industrial use (Masindi et al., 2022b). The same authors explain how the treatment of mine wastewater can lead to the reclamation of drinking water making it a zero-liquid discharge process. After the AMD minerals have been recovered, the pre-treated water can go via reverse osmosis to reclaim drinking water in accordance with SANS 241 (Akinwekomi et al., 2020). Pino et al. (2020) investigated the recovery of water on a pilot-scale through the optimization of nanofiltration for AMD treatment. According to their study, the authors have indicated that up to 80% of the water can be recovered through nanofiltration. This will minimize the use of freshwater resources. Aguiar et al. (2016) evaluated membrane separation treatment of gold AMD. After mineral recovery using nanofiltration and reverse osmosis 60% of water was recovered at optimized conditions. (Wang et al., 2021) also recovered 60% of water in their study. The authors demonstrated the use of direct contact membrane distillation to recover water from AMD. The results from this study demonstrated 60% of water recovery and 22% flux reduction. (Masindi et al., 2018b) reclaimed water after treating AMD with magnesite, lime, and CO_2 bubbling (MLC). The results from this study indicated that most of the components were within the DWS limits though the water needed further treatment for consumption. Masindi (2017a) examined the recovery of drinking water from AMD. The author discovered that the drinking water could be successfully reclaimed using a reverse osmosis system. The pH of the drinking water obtained in this method was around 6.5, and the metal removal rate was approximately 100%, meeting SANS 241 drinking water quality regulations. Furthermore, Buzzi et al. (2013) evaluated the use of electrodialysis as a suitable technology to recover water from coal AMD. To investigate the effectiveness of this technology, three AMD were treated, and the findings indicate that electrodialysis is suitable for recovering water from AMD, with desirable pollutant removal efficiency $\geq 97\%$. Nleya et al. (2016) also claimed water during the recovery of sulphuric acid.

2.4 Beneficiation and valorisation of recovered minerals

2.4.1 Fe-based coagulants

The elimination of turbidity, colour, odour and taste are mostly accomplished by the removal of suspended solids, which are aggregated through the necessary mechanism of coagulation (Tzoupanos and Zouboulis, 2008). Coagulants are crucial in the process of water treatment as they are used to remove suspended solids from drinking water. Ferric chloride and ferric sulphate have been widely used in water and wastewater treatment with the main quest of reducing turbidity, colour, metals and other contaminants. According to Brandt et al. (2017), ferric chloride is preferred for being applicable in a broader pH range. Commercial grade Fe(III) and sulphuric acid are mainly used for the production of ferric chloride. However, recent research has focused on the use of waste materials instead of dwindling virgin materials. For example, Menezes et al. (2010) produced poly-alumino-iron sulphate from AMD by chemical precipitation. The Fe(II) was converted to Fe(III) by aerating AMD for 24 h at pH 2.5- 3.0.The potassium dichromate method was used to monitor ferrous iron and aluminium were precipitated as metal hydroxide by increasing and maintaining pH at 5.0 ± 0.1 with addition of 4 mol/L NaOH solution. The metal hydroxide was separated at 3000 rpm by centrifugation. The precipitate was dissolved in sulphuric acid to produce sulphate-based coagulants and achieve solution coagulant which comprises of 72% ferric iron and 27.5 % aluminium. The recovery was 97% for iron and 99% for aluminium, resulting in a reduction in sludge volume of 98%. The results from this study indicate that the recovered Fe(III) from AMD can be used to produce coagulant for water treatment. The initial turbidity was 81.3, after treatment with the synthesized coagulant it was 0.5 which is 99.3% removal efficiency. Subsequently, Menezes et al. (2009a) produced poly-ferric sulphate coagulant from coal AMD by selective precipitation of iron. Fe(III) was precipitated at pH 3.8, which was followed by dissolution in sulphuric acid. The results from this study coincided with literature. Another study conducted by Almeida and Schneider (2020) to produce ferric chloride from iron ore tailing for coagulation purposes. HCl concentration, heating time and temperature were investigated. The results indicated that the leaching of iron ore tailing was carried out at temperature of 80℃ for 120 min with 10.8 mol L^{-1} of HCl. This resulted in 94% solubilization efficiency of iron. The water treatment results indicated the effectiveness of the coagulant in removing turbidity by ≥98% from raw water. The valorisation of recovered Fe(III) from AMD reduced the pressure on virgin materials used for the production of ferric coagulants. AMD serves as a source of feedstock for coagulants. Mwewa et al. (2019b) conducted a study on the synthesis of poly-alumino-ferric-sulphate coagulant from AMD by precipitation. The authors indicated the experimental condition as follows; the co-precipitation of iron and aluminium was done using sodium hydroxide at pH values 5.0, 6.0 and 7.0 to evaluate the recovery of iron and aluminium as hydroxide precipitates. The recovery of iron and aluminium was 99.9% and 94.7% respectively at pH 5.0. In order to produce the coagulant, the precipitate was dissolved in 5.0% (w/w) sulphuric acid. The results demonstrated 91.9 % turbidity removal and 56% COD removal for the brewery wastewater treatment. On the other hand, (Lopes et al., 2011) investigated the use AMD with high Fe content as a coagulant to treat wastewater. For coagulation, 15 mL of AMD was added to 1L of sewage at optimum condition. The results demonstrated 74%, 62%, 65% and 97% removal efficiency for suspended solids, COD, BOD_5 and phosphorus, respectively. For Fenton's Reaction, 15 mL of AMD was added into 1 L of sewage and Fenton's Reaction was conducted over 3 hours. The results showed that COD and BOD_5 removal were higher than the coagulation studies. This resulted in 78%, 80%, 80% and 92% for suspended solids, COD, BOD_5 and phosphorus. Moreover, (Yang et al., 2021) investigated the production of P-doped poly-ferric chloride (PPFD) coagulant from pickling sludge. Fe was extracted by two-step extraction and oxidised with $\mathrm{H_2O_2}$. The coagulant was prepared using $\mathrm{Na_2HPO_4}$. The synthesized PPFD was used to treat wastewater with main constituents being colour and COD. Under optimal conditions, the removal efficacy of colour and COD were 96.25% and 69.91%, respectively.

2.4.2 Fe-based adsorbent

Adsorbent is a solid material utilized for the removal of pollutants from liquid or gas that could affect the environment. Various commercial adsorbents such as activated carbon, zeolites, silica gel and activated alumina are vastly utilized. Recent research has shown that iron-based adsorbents, which are non-toxic, inexpensive and are readily available in large quantities, offers promising outcomes for the removal of contaminants in water and the preservation of the environment. Due to their high surface area, high number of surface-active sites, and strong magnetic characteristics, iron nanoparticles have high adsorption efficiency, high contaminant removal rates, and fast and quick magnetic field-mediated separation of adsorbent from solution (Simate and Ndlovu, 2014, Rodríguez-Galán et al., 2019). Their use as adsorbents have successfully been indicated by Li et al. (2016) on the removal of phosphate from wastewater by metal oxides and hydroxides adsorbents. Muedi et al. (2022) evaluated the use of Fe/Al di-metal nanostructured composite synthesized from Fe(III) and Al(III) recovered from AMD for adsorption of Congo red dye from aqueous solution. The results indicated ≥ 99% removal efficacy for Congo red dye and high Langmuir adsorption capacity of 411 $mg \cdot g^{-1}$. These Fe-based adsorbents can be sold to different industries and for different purposes. Iron oxide particles recovered from AMD can be used as adsorbents to remove contaminants from wastewater (Yuan et al., 2022). Metal oxide-based nanomaterials pose efficiently as adsorbents due to their high sorption capabilities (Ansari et al., 2023). The remediation of contaminants in water, such as arsenic, chromium, phosphate, chloro-organics, and waterborne bacteria (e.g., *E. coli*), have been achieved by adsorption or dechlorination procedures by employing iron and iron oxide nanoparticles synthesized from diverse processes (Cross et al., 2014). The recovered Fe from AMD can be used for the synthesis of hematite which can be applied for the treatment of AMD. Akinwekomi et al. (2020) investigated the recovery of Fe-species from coal acid mine drainage, and a selective and fractional precipitation process did the recovery The recovered Fe-species showed a very high purity (>99%) and were used to synthesis hematite at 700 ˚C for 45 min. The high purity suggest that the hematite can be used for industrial application such as adsorbents in water treatment. This can reduce industries' use of virgin materials. Iron is found in elevated levels in AMD produced acicular goethite nanoparticles (AGNs) from AMD on an industrial scale. This can be used in water treatment for adsorption of phosphates, arsenate, and humic acids.

2.4.3 Fe-based pigment

Fe can be recovered in multiple ways from AMD and beneficiated in different ways depending on the desired end-product. It can be recovered to create commercially viable iron oxides as a raw material for the production of pigments, ceramic additives, and so on. The recovery of Fe from AMD is very advantageous as it reduces toxin, and it is more amenable to recovery and reuse. The recovered Fe can be utilized for pigment production as indicated in literature (Akinwekomi et al., 2017, Akinwekomi et al., 2020). Ryan et al. (2017) studied selective precipitation procedures utilised to recover iron oxides from mine water to produce paint pigments. Oxidation, pH modification, and filtration were used in a stepwise selective precipitation procedure. Iron oxides precipitated at pH 3 exhibited the highest purity and possessed a unique yellow colour reminiscent of jarosite. Magnetite material has been widely employed in several sectors due to its chemical composition, structure, and magnetic capabilities. It can be used as a raw material to produce both of metallic iron and paints. In paints, varnishes, clay, and coloured concrete, goethite can be utilised as an affordable, longlasting pigment (Mohan and Pittman, 2007, Silva et al., 2012b, Masindi et al., 2022b). Tabak et al. (2003) recovered metal precipitate and converted them into marketable pigments.

2.4.4 Fe-based catalysts

Fe-based catalysts are considered to have low cost and low toxicity, with various valence states. Iron oxide particles recovered from AMD can be used for the production of reasonably high purity magnetite or goethite (Flores et al., 2012). New methods have been proposed to synthesis valuable minerals and treat AMD. (Sun et al., 2015) evaluated a new air-cathode fuel cell installation for the in-situ synthesis of heterogeneous electro-Fenton catalysts in AMD. The synthesized AMD was used to create three different types of nanostructured iron oxide/graphite felt composites: FeOOH/GF, Fe2O3/GF, and Fe3O4/GF. The results from this study showed that when Rhodamine B (Rh B) was used as the test pollutant, the removal rates of Rh B of the three composites were 62.5%, 95.4%, and 95.6%, respectively, under neutral pH conditions. On another study, (Sun et al., 2018) employed the air-cathode fuel cell (AC-FC) technique for the fabrication of iron oxide/carbon composite with electron-Fenton (ET) catalyst using Fe(II) in AMD. This paper investigates the effect of coexisting cationic metals other than Fe^{2+} in AMD on ET catalyst fabrication process. After that, the AC-FC was used to decompose organic contaminants in the actual AMD. The test findings showed that the AC-FC performed well in treating genuine AMD, and the treated wastewater met the prescribed discharge standards. Meanwhile, Fe^{2+} ions were recovered from genuine AMD and used as a material source for the heterogeneous electro-Fenton catalyst, allowing for the efficient usage of valuable resources in AMD and conforming to the notion of green sustainable development. It is worth noting that these iron oxide particles can be employed in pigments and other products, making the procedure environmentally friendly. According to Lappas et al. (2016) recovered iron can be used as fused iron catalysts which are prepared by fusion. Mostly iron based catalysts are utilised in both low temperature Fischer-Tropsch and high temperature Fischer-Tropsch process mode (Olah and Molnár, 2003, Lappas et al., 2016). This was supported by Bromfield and Vosloo (2003) on the study of Sasol when it developed a new Fe-based catalyst for the high temperature Fischer-Tropsch process. Lefèvre and Dodelet (2003) evaluated the use of Fe-based catalysts for the reduction of oxygen in polymer electrolyte membrane fuel cell conditions. Fe recovered and synthesized as ferric chloride can be used as Lewis's acids for the production of printed circuit boards. AMD under circular economy is viewed aa a secondary source for mineral recovery and valorisation. A study conducted by Aslam et al. (2023) to valorise AMD into an Iron catalyst to treat municipal wastewater using solar photo-Fenton.

The authors utilised both iron-rich liquid AMD and synthesized magnetite, hematite, and goethite. AMD-recovered catalysts and iron-rich AMD were added in wastewater to initiate solar photo-Fenton process for COD removal. The experiments were carried out separately for both catalysts. The COD removal reached 99% for iron-rich AMD at the following conditions, 1000 mg/L H_2O_2 at pH 2.8. It was observed that under the same conditions COD removal was 35%, 25% and 7% for hematite, goethite, and magnetite, respectively. The results from this study indicate that AMD iron-rich was observed have higher COD removal efficiency than AMD synthesized catalysts.

2.4.5 REEs

Due to challenges in the exploration and mining of REEs, mine tailings seems to be a promising resource for REEs (Balaram, 2019). Given the importance of these minerals and the requirement for a reliable domestic supply, current research aims to use AMD as an alternative secondary resource for REE The benefits of the recovered REEs from AMD still need to be investigated as there is minimal work to be done on its application after recovery.. However, Hermassi et al. (2022a) conducted a study on the recovery of REEs from mine water and by separating the REE from metals. The recovered REEs were used as REE- phosphates. The recovered REE are good as fertilizers. This was demonstrated by (Xu et al., 2003a), Xu et al. (2003b) utilising recovered REEs as a mixture to improve crop production. Applying rare earth element mixes at >10 mg kg−1 soil, this resulted in a considerable rise in the concentrations of light rare earth elements in the roots, and at 50 mg kg−1 soil, a similar occurrence was detected in the plant tops. Lanthanum alone, at a dose more than 10 mg La kg−1 soil, resulted in a considerable rise in La content in plant roots and crowns. The content ratio of La to Ce in maize plants appeared to rise as the application doses of rare earth element(s) increased. Another study conducted by (Wen et al., 2001b), Wen et al. (2001a) to examine the distribution and bioaccumulation of recovered REEs in wheat, rice, and vegetables grown in Jiangxi, Anhui, Beijing, and Heilongjiang provinces in southern and northern China following varied levels of REE fertilizer application. The study found that REEs accumulate in plants in the following order: root, leaf, stem, and grain. Applying REE fertilizers significantly increases REE concentrations in roots, leaves, and stems. (Zhang and Shan, 2001) conducted a greenhouse study to investigate the accumulation of REEs such as La, Ce, Pr, and Nd in winter wheat (*Triticum aestivum L.*), as well as the speciation of these elements in soil after applying REE-based fertilizers. The experiment confirmed improved agricultural yields. The accumulation patterns of Pr, Nd La, and Ce, in wheat were dependent on the concentration of REE fertilizer applied. Specifically, the accumulation increased as the REE concentration in the fertilizer increased at low application rates, remained constant within the medium REE range, and decreased as the REE concentration increased at high application rates. The studies above demonstrate that the recovered REEs can be used as fertilizers to improve agriculture. Li et al. (2012) examined the application of hydrous cerium oxide nanoparticles for the adsorption of arsenic. Hydrous cerium oxide (HCO) nanoparticles were synthesized by a straightforward precipitation technique, and their ability to adsorb arsenic was investigated. HCO nanoparticles exhibited outstanding adsorption characteristics on both As(III) and As(V) owing to their substantial specific surface area of 198 m2/g and the presence of surface hydroxyl groups with strong affinity. Under neutral pH conditions, the HCO compound demonstrated an arsenic adsorption capability surpassing 170 mg/g for As(III) and 107 mg/g for As(V). The HCO nanoparticles demonstrated a remarkable arsenic adsorption capability absorbing more than 13 mg/g of As(III) and As(V) at a concentration of 10 μg/L, 40 mg/g at concentration of 50 μg/L. This surpasses the arsenic adsorption capabilities of the majority of commercially available adsorbents. To date, there has been a lot of research studies done on the recovery of REEs but very limited studies on the use of the recovered REEs.

2.4.6 Sulphate

Sulphate present in AMD is found in elevated concentration making it viable for the recovery and reuse. The recovered gypsum can then be used for road construction, production of bricks, and production of geo-polymer bricks, amongst others. This further demonstrate the circularity of the mine water management initiatives and their contribution towards zero waste, i.e., liquid and solids, emissions (Nleya et al., 2016). Furthermore, solidified gypsum can serve as construction material. The procedure has the potential to minimize the waste by allowing the sludge to be utilized as a substitute for lime treatment(PreuB et al., 2012b, PreuB et al., 2012a). Nleya et al. (2016) demonstrated that the sulphuric acid recovered can be sold to create revenue which can offset some of the operational cost. Globally, sulfuric acid is utilized as a catalyst in the manufacturing of gasoline, jet fuel, and polymers (Wagenfeld et al., 2019). Most of sulphur is imported in Africa and this has resulted in inflated cost due to its transportation while it is a cheap product.

Sulphuric acid has vast applications and its recovery making economically viable for beneficiation. Sulphuric acid can be used in leaching. (Zhao et al., 2014) used sulphuric acid when leaching out chromite. It was also utilised by (Venter and Boylett, 2009) when investigating different oxidants during leaching of uranium. It can also be used to regenerate ion exchange resin; this observation was made by during the removal of metals from AMD. The recovered sulphuric acid can be utilized for the production of phosphoric acid, hydrochloric acid, and nitric acid. Sulphuric acid is also used for fertilizer production (Saeid and Chojnacka, 2014), lead-acid batteries, pigments, and dyes, and it also serve as a reagent in the paper, petroleum, and metal sectors. Additionally, It finds applications in the pharmaceutical industry, as a food additive, and as a cleanser for toilet bowls.

2.4.7 Beneficiation of AMD

While researchers have been focusing on the beneficiation of minerals recovered from AMD, new developments have been made to beneficiate AMD itself. (Aslam et al., 2023) used real AMD to treat municipal wastewater. As alluded to above, the results from this study indicated that AMD iron-rich was observed to be more effective in treatment of municipal wastewater as compared to AMD synthesized catalysts. Bai et al. (2021) examined the process by which lime-depressed pyrite flotation is activated by introducing AMD in order to substitute current activators and transition towards a more environmentally friendly method of producing copper sulfide ore. Increasing the volume ratio of AMD to high alkali system to 3:1 improved the flotation recovery of pyrite, which was hindered by lime, by 64% in pure mineral flotation tests. Empirical ore testing confirmed AMD's capacity to induce pyrite flotation using the SBX collector. Consequently, the utilization of AMD in pyrite beneficiation can not only decrease the reliance on chemical reagents but also provide an innovative method for the sustainable treatment of AMD. Huang et al. (2020) conducted an experiment for the removal of ciprofloxacin (CIP) using AMD rich in iron and manganese in electron-Fenton cathode. In 60 min under optimal conditions, 89% CIP removal efficiency was achieved. This opens up new avenues for organic pollutants removal using AMD. Salama et al. (2015) explored the innovative application of AMD for the retrieval of biomass from two microalgae species with distinct morphologies. The study examined the effects of varying AMD dosage, microalgal cell density, and medium pH. Scenedesmus obliquus and Chlorella vulgaris formed aggregates most effectively when exposed to a 10% AMD solution at an initial pH of 9, regardless of the cell density of 0.5 and 1.0 g/L. S. obliquus had a flocculation efficiency of 89% whilst C. vulgaris demonstrated a higher efficiency of 93%. The zeta potential (ZP) of S. obliquus increased from -10.66 to 1.77 while the ZP of C. vulgaris increased from -13.19 to 1.33, respectively.

2.5 Factors hampering the recovery and beneficiation of minerals.

Although beneficiation of minerals is essential, literature has demonstrated some of the challenges associated with it, the major one being co-precipitation of impurities. Literature has indicated that recovery of Fe by precipitation results in co-precipitation with other metals. Rao demonstrated co-precipitation of dissolved metal ions of ferric hydroxide precipitation during the study of AMD as a coagulant. carried out research to recover rare earth elements from bastnaesite that had been pre-concentrated. Reasonable purification of rare earth elements from iron, aluminium, magnesium, and thorium was discovered by the writers. The concentration of several of the minerals in AMD is another factor impeding their recovery.

. Some minerals are present in low concentrations which makes them difficult to recover. The use of membrane filtration results in fouling of the membrane which hampers the recovery of minerals. Buzzi et al. (2013) indicated that the deposition of iron on the surface of the cation-exchange membrane leads to membrane blockage as a result of scaling, resulting in a drop in process efficiency. Membrane separation technique offers the benefit of producing clean return water of superior quality. However, it also presents certain disadvantages, including the need for significant energy input, limited water permeability, frequent membrane fouling and limited operational lifespan, as well as high operating expenses. As a result, recovering water from AMD is a challenging process, with several approaches having differing strengths and limitations. Oh et al. (2016) discovered some small amounts of impurities during the recovery of metals in their studies.

2.6 Economic viabilities

Fe is found in high concentrations in AMD which makes it economically viable to recover and reuse it. Hu et al. (2022) conducted an economic feasibility analysis during their pilot-scale study on the treatment and recovery of iron from AMD. The analysis indicated that the recovery of Fe from AMD is cheaper than the traditional lime neutralization. Their study demonstrated that 0.144 USD per m^3 of AMD treated can be saved, which can further save about 12.91 million USD in sludge treatment. Furthermore, Le et al. (2020) conducted the economic assessment in their study to recover Fe(III) and Al(III). The authors indicated the total profit made per m^3 of AMD to be 1.31 USD, 1.946 USD from iron product. The analysis indicates that this saved 2.05 USD on the wastewater treatment cost. In the acid upgrading process, useful water could also be obtained. An economic analysis of the proposed process revealed that money from sulphuric acid may be utilized to offset some of the operational costs.

2.7 Feasibility of using Fe(III) for drinking water treatment

Drinking water handling facilities use ferric chloride to produce coagulants for drinking water treatment. The primary aim of the coagulant is to reduce the NTU of the water which is caused by suspended and dissolved substances. To fit this context, a succinct distil of the drinking water process is summarised as follows:

2.7.1 Chemical dosing

Chemical dosing is usually the first step in water treatment whereby coagulants such as alum, ferric salts or polymers are added in water to destabilize the negative charge of suspended contaminants by neutralization and adsorption (Brandt et al., 2017). It also bound together destabilized particles by enmeshment in a sweep floc. The main purpose of this stage is to form floc big enough to settle at the sedimentation tank. Subsequently, ferric chloride consumes alkalinity so the addition of lime as a coagulant aid is essential for regulating the pH of the water. If the pH is not controlled and drops too low, the insoluble ferric ion (Fe(III)) will convert to soluble ferrous ion (Fe(II)) resulting in brown water. Polymers, on the other hand, are cationic and does not affect the pH of the water which requires low lime dosages, and they produce much lesser sludge but at an expense of cost because of their high price as compared to Fe(III).

2.7.2 Sedimentation

Sedimentation is the removal of settleable solids by gravity, this process takes place in a round, rectangular, or square sedimentation or settling tank. This is the step between flocculation and filtration where floc formed during coagulant dosage are allowed to settle at the bottom and collected as sludge regularly for the efficiency of the process. Effective sedimentation depends entirely on the coagulation-flocculation process and on the design of the sedimentation tank (Guo et al., 2014).

2.7.3 Filtration

Filtration is used for the removal of suspended solids from water. This is a subsequent step after sedimentation or dissolved air floatation. Water passes through filter media to remove fine particles that did not settle in the sedimentation tank (Brandt et al., 2017). Entrapment of fine particles will also reduce significant number of bacteria but insufficient to render the water suitable for consumption (Verma et al., 2017). They are usually two types of filters used in water treatment, slow sand filters which utilizes sand only as a filter media and another type is rapid filters, commonly referred to as multimedia filters which comprises sand, anthracite, granular activated carbon and other media (Verma et al., 2017).

2.7.4 Chlorination

Chlorination is usually the last stage of the water treatment as it is utilized for the disinfection of the water. This stage is designed to eliminate any surviving pathogenic bacteria and viruses and as a preventative measure to avoid the regrowth of bacteria in the distribution systems. The chlorine gas is added into the water under pressure before the distribution of the water to the end-users.

2.8 Types of coagulant used in drinking water treatment.

The elimination of turbidity, colour, odour and taste are mostly accomplished by the removal of suspended solids, which are aggregated through the necessary mechanism of coagulation (Tzoupanos and Zouboulis, 2008). Coagulants are crucial in the process of water treatment as they are used to remove suspended solids from drinking water. Coagulation is a process in which chemical compounds are added to the water, to destabilize the negative charges on the particles suspended in water. It is usually achieved using polymers, aluminium, and iron-salts. There is a compelling need to improve and optimize operational performance of water treatment facilities to reduce costs as a result of increased operational costs and strict administrative requirements from SANS 241. There are two types of chemical coagulants for water treatment: organic and inorganic.

2.8.1 Inorganic coagulants

The most widely utilised inorganic coagulants in the water treatment sector are salts of aluminium and iron. These include iron-based metals (ferrous sulphate, ferric chloride, and ferric sulphate) and aluminium-based metals (aluminium chloride, aluminium sulphate, sodium aluminate) (Bolto and Gregory, 2007). The inorganic coagulants are easy to handle and to apply and sometimes produced lesser sludge. Tetteh et al. (2019) reported that some are effective in hard waters at low coagulant dosages and ferric salts are effective at pH between 4.0 and 11. Furthermore, ferric chloride encourages faster sedimentation.

2.8.2 Organic coagulants

Organic coagulants are liquid compounds with high coagulation efficiency because of the structure of their polymers and the potency of their cationic charges. Organic coagulants are often employed to reduce sludge development and solid-liquid separation The following chemicals form the foundation of organic compositions, polyamines and poly-DADMACs, which works solely by charge neutralization (Bolto and Gregory, 2007). Organic polymers are usually used as coagulant aid. Since organic polymers are naturally relatively viscous liquids, it can occasionally be difficult to disperse them evenly throughout a medium. Organic coagulants do not consume alkalinity from the medium, which significantly reduces pH and conductivity fluctuations. There are three types of polymers: cationic, anionic, and non-ionic polymers.

2.8.3 Cationic polyelectrolytes

Positively charged organic coagulants with natural or synthetic bases are referred to as cationic polymers. Despite pH variations, several polymers carry charge ammonium groups, making them strong electrolytes (Tzoupanos and Zouboulis, 2008). Cationic polymers are widely preferred because they have a positive electrical charge and water comprises negatively charged particles. They are used to neutralize negatively charged particles and allow particles to stick together to form flocs.

2.8.4 Anionic polyelectrolytes

When the ionic group of anionic polymers dissolve in a medium, they become amphoteric polymers, which acquire a negatively charged ions which are used to remove positively charged solids (Tzoupanos and Zouboulis, 2008). Anionic polyelectrolytes are utilized in conjunction with aluminium and iron coagulants. They have the advantage of increased floc size, improved settling, and stronger flocs. They are not materially affected by pH, alkalinity, hardness or turbidity (Taghizadeh et al., 2020)

2.8.5 Non-ionic polyelectrolytes

Polymers with a balanced, or neutral, charge are known as non-ionic polyelectrolytes. Upon dissolution, they liberate both cations and anions, which can have positive and negative charges, respectively. Non-ionic polyelectrolytes are less expensive even if they must be introduced in higher dosages than other kinds (Churchman, 2002). The dosages of polyelectrolytes are incredibly low when compared to other coagulant aids.

2.9 Ferric chloride production process

The traditional method for manufacturing ferric chloride involves the formation of ferrous chloride by attacking iron with HCl.

$$\mathrm{Fe + 2HCl \rightarrow FeCl_2 + H_2} \qquad 2.5$$

Through chlorination, the obtained ferrous chloride is converted to ferric chloride.

$$\mathrm{2FeCl_2 + Cl_2 \rightarrow 2FeCl_3} \qquad 2.6$$

The concentration of $FeCl_3$ used in the preparation of concentrated solution is 35 to 45% by weight. This process is explicitly described in the European patent EP0493023B1, i.e., the developed invention or method relates to a method for the preparation of anhydrous ferric chloride from a dilute ferrous or ferrous-ferric chloride solution Another method is to produce ferric chloride using a mixture of ferric and ferrous oxides (Almeida and Schneider, 2020).. The application of a solution containing 32% hydrochloric acid, followed by the introduction of chlorine gas, leads to the production of ferric chloride as a result of the subsequent chemical reactions. (Abdel-Fatah et al., 2021):

$$\mathrm{Fe_2Cl_3 + 3HCl \rightarrow 2FeCl_3 + 1.5H_2} \qquad 2.7$$

$$\mathrm{FeO + 2HCl \rightarrow FeCl_2 + H_2O} \qquad 2.8$$

$$\mathrm{FeCl_2 + 0{,}5Cl_2 \rightarrow FeCl_3} \qquad 2.9$$

2.9.1 Thermal process

Thermal processes are non-catalytic reactions that utilises heat application to mix, rearrange or breakdown molecules. Specifically, Fe species react with dry chlorine at temperature between 500℃- 700℃ on a thermal process to produce ferric chloride. The precursors that are used comprise Fe and Cl ions. Herlitschke et al. (2016) to evaluate the utilization of Fe(III) and Cl_2 for the synthesis of ferric chloride. The authors of the study indicated that the of ferric chloride product was prepared by subjecting Fe to high temperatures in an anhydrous Cl_2 gas stream. The production of anhydrous Cl_2 gas was achieved through the oxidation of concentrated hydrochloric acid with $KMnO_4$. The Cl_2 gas stream was purified by rinsing it with H_2O to remove excess HCl, dried over concentrated H_2SO_4, and subsequently passed over Fe pieces heated at 250 ◦C in inert atmosphere. $FeCl_3$ was collected as a dry, shiny violet powder. Knuuttila et al. (1994) reported the production of ferric chloride via the reaction of scrap iron with HCl, which is then oxidised using oxygen gas and evaporated water specifically at 65–82° C is the ideal raised temperature range. Furthermore, larger concentrations are obtained by evaporating water under high heat to enhance the total iron concentration, but this method is prohibitively expensive. In essence, thermal processes produce ferric chloride of high purity, but high energy is required for the production process hence making it energy and chemical hungry.

2.10 Production of ferric chloride from iron ore tailing

For the production of ferric chloride, synthetic/commercial Fe(III) is reacted with hydrochloric acid to produce ferric chloride following the illustration demonstrated in **Figure 2.1**.

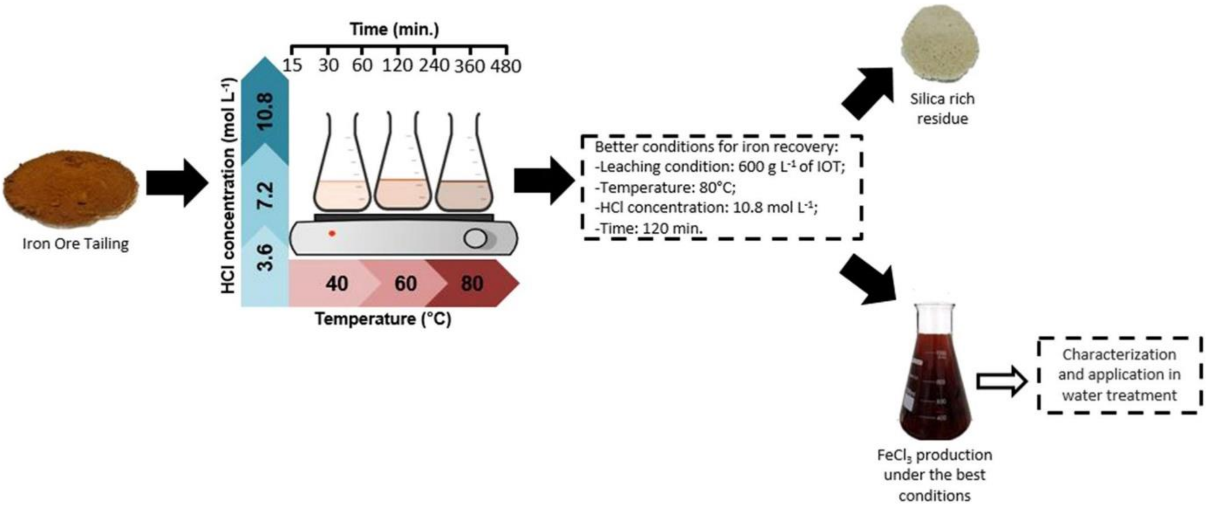

Figure 2.1: The ferric iron production process

As depicted in **Figure 2.1**, this process indicates the benign production of ferric iron from iron ore tailing. Therefore, this demonstrates the feasibility of recovering Fe(III) from acid mine drainage and its application for the production of ferric chloride. This will be a novel approach towards the beneficiation of Fe(III) recovered from AMD.

2.11 Summary of the literature review

Since the Covid-19 pandemic attacked the world, the prices of monomers have increased drastically causing the water and wastewater treatment industries to resort to the use of ferric compound, which are cheaper and abundant. However, their over-exploitation and fear for their depletion is at stake. The recovery of minerals from AMD is essential in circular economy. The recovery of Fe(III) from acid mine drainage and its application as a coagulant has been explored to a limited extend, as such, this study is the first, according to the author's knowledge, to explore its feasibility as a coagulant for drinking water treatment and explore the potential toxicity of using it in water treatment due to precipitation of metals. The recovery and reuse of Fe from AMD can resolve potential environmental problems. Traditionally, AMD treatment systems have been established, but they are limited by cost considerations, handling processes, and the production of hazardous secondary sludge that needs specialised disposal facilities that are expensive to maintain. The recovery and beneficiation of these minerals will play a huge role. Lately the water and wastewater industries have been facing a huge problem due to shortage of coagulants. Thus, recovery and beneficiation of minerals will go a long way in addressing such issues.

CHAPTER THREE

MATERIALS AND METHODS

In this chapter, acquisition of the samples, experimental configurations, optimisation studies, and analytical techniques used to fulfil the goals and objectives of this study are meticulously explained. The quality control procedures and simulation conditions applied in the experiments are also described in this section.

3.1 Acquisition of the samples

Real AMD was collected from the heap (toe seep) of an active mine from Mpumalanga province, South Africa, using 25 L high density polyethylene (DHPE) containers (jerry cans). Before collection, AMD was pre-filtered using Macherey Nagel MN 615-Ø125 mm filter papers to remove debris and suspended solids and the filtrate was then moved and stored in the laboratory at 4°C, until use for Fe(III) recovery experiments. Raw water was collected from an abstraction point from Wilge River that feeds a water treatment plant in Gauteng Province, South Africa. Similarly, 25 L HDPE jerry cans were used for river water collection and the collected water was stored at the laboratory at 4°C, before being treated with $FeCl_3$. Finally, municipal wastewater was collected from two wastewater treatment plants (WWTP-A and WWTP-B) in Gauteng Province, South Africa. Again, municipal wastewater was collected using 25 L HDPE jerry cans, pre-filtered through Macherey Nagel MN 615-Ø125 mm filter papers, and stored at 4°C, before being treated with $FeCl_3$.

For Fe(III) selective precipitation and recovery from AMD, MgO was used. This was produced by calcining locally available magnesite, which was hand collected from a derelict magnesite mine in Folovhodwe, South Africa, as described elsewhere (Masindi et al., 2018c). For $FeCl_3$ production from the recovered Fe(III) sludge, the direct chlorination process was used. To this end, industrial grade hydrochloric acid (HCl) (30%) was procured from Sigma Aldrich and reacted with Fe(III) as described elsewhere (Almeida and Schneider, 2020). Finally, to assess the efficiency of the AMD-synthesized $FeCl_3$ as a coagulant for water and wastewater treatment applications, its efficacy was identified and compared to the efficacy of commercially available $FeCl_3$, when treating the same aqueous matrices. For this reason, commercially available $FeCl_3$, which is already being used by South African water and wastewater industry, was procured from Protea chemicals (Pty) Ltd.

3.2 Ferric iron recovery

For Fe(III) recovery from the coal mine AMD, selective precipitation, as described in (Masindi et al., 2018c), was employed. Specifically, the pre-filtered AMD was transferred into a borosilicate laboratory reactor and was dosed with a predefined mass of MgO to increase the pH to 3.5, where Fe(III) commences to precipitate. Specifically, the AMD-MgO mixture was stirred for 30 min, at 500 rpm using an overhead stirrer, and was left to settle out for 30 min to separate the precipitate (Fe(III)-rich sludge) from the supernatant (Masindi et al., 2018c). This pH value, i.e., 3.5, is fairly similar to the one employed by (Menezes et al., 2009b), i.e. 3.8, to recover Poly-Ferric Sulphate (PFS) from coal mine AMD when using NaOH. However, in our case study MgO was used instead of NaOH which avoids the sulfate co-precipitation. The precipitate was then dried in the oven at 105 ℃ for 24 hours and stored until utilization for $FeCl_3$ production.

3.3 Ferric chloride synthesis

The targeted ferric salt herein is $FeCl_3$ and for its production the recovered Fe(III)-rich sludge was reacted with industrial grade HCl towards $FeCl_3$ synthesis (AMD-synthesized $FeCl_3$ thereafter). Specifically, following Almeida and Schneider (2020), 0.01 mol of HCl was added into a volumetric flask filled with deionised water to prepare a 0.001 M solution. Then, the Fe(III)-rich sludge was added and mixed, using a magnetic stirrer, for 30 min to synthesize $FeCl_3$. Finally, 0.7 mL of the $FeCl_3$-rich solution was added into a 1 L volumetric flask fill with deionised water to prepare the stock solution that was used in the coagulation studies.

3.4 Characterisation

3.4.1 Elemental composition of the Fe(III)-rich sludge recovered from AMD.

A detail characterization of both the MgO (and its parent material) as well as of the recovered Fe(III) can be found in , as described in (Masindi et al., 2018c), the magnesite samples underwent a milling process for 15 minutes at a speed of 800 revolutions rpm using a Retsch RS 200 vibratory ball mill. Subsequently, the milled materials were filtered through a screen with a particle size of 32 micrometres. The samples underwent calcination at a temperature of at least 900 °C using a blast furnace for a duration of 1 hour. The samples were stored in a hermetically sealed plastic bag until they were used to extract metals. Therefore, here focus is placed on its chemical composition, which will provide insight about possible impurities in its matrix. To this end, the X-ray fluorescence (XRF) (Thermo Fisher ARL-9400 XP Sequential XRF equipped with Win-XRF software) analytical technique was employed. The samples underwent a drying process at a temperature of 100℃ and were subsequently subjected to roasting at a temperature of 1,000℃ in order to estimate the loss of ignition (LOI) for elemental analysis using XRF.

3.4.2 Characterisation of aqueous samples

For the characterization of the aqueous samples under study (raw and $FeCl_3$ treated water/wastewater) a multi-parameter probe (Hach Company HD40D) was used to measure the pH and electrical conductivity (EC). Turbidity was recorded using a tungsten lamp turbidimeter (Hach Company TL2350). Metal and non-metal fractions were determined using inductively coupled plasma mass spectrometry (ICP-MS) (Thermo Scientific XSERIES 2 ICP-MS, coupled to ASX-520 auto sampler) and inductively coupled plasma - optical emission spectrometry (ICP-OES) (Agilent Technologies 5110 ICP-OES coupled with SPS 4 auto sampler), as required based in their concentrations.

3.5 Optimization studies

Optimization studies were carried out to determine the optimum water treatment conditions when using the AMD-synthesized ferric salt ($FeCl_3$). Specifically, the effect of $FeCl_3$ dosage, mixing speed, and contact time (mixing duration) on contaminants removal from the collected raw (river) water was examined. For this reason, batch experiments were conducted in the laboratory using the one-factor-at-a-time (OFAT) method. Specifically, changes in the pH were recorded, while the removal efficiencies (%) for Al, chromium (Cr), colour, copper (Cu), Fe, Mn, nickel (Ni), and zinc (Zn) were calculated using Eq. (1):

$$\text{Removal (\%)} = \frac{\mathrm{C_{initial}} - \mathrm{C_{final}}}{\mathrm{C_{initial}}} \times 100 \qquad (1)$$

where $\mathrm{C_{initial}}$ the initial concentration of the examined contaminant/indicator and $\mathrm{C_{final}}$ the final concentration of the examined contaminant/indicator.

3.5.1 Effect of dosage

A volume of 1000 mL of the aqueous solution was added into six 1000 mL beakers. Different volumes of the Fe(III) solution (0.1 – 8 mL) were added into the same beakers. The mixtures were mixed for a period of 60 seconds at 200 rpm by utilizing a jar test stirrer. Thereafter, the samples were afforded 60 minutes for the suspended solids to settle. The turbidity of the settled supernatant was determined. The supernatant was filtered using Whatman gravity filter. The determination of pH, electrical conductivity and turbidity was performed on the raw, settled and filtrate solutions. The same conditions and procedures were used for commercial ferric compound and the performance of the two solutions was compared.

3.5.2 Effect of mixing speed

A volume of 1000 mL of raw aqueous solution was added into six 1000 mL beakers, into which 0,2 mL of the synthesized solution was added. The mixtures were mixed for 1 minute each at different mixing speeds (25, 50, 100, 150, 200 and 250) rpm by utilizing a jar test stirrer. Thereafter, the samples were afforded 60 minutes for the suspended solids to settle. The supernatant was filtered using Whatman gravity filter. The determination of pH, electrical conductivity and turbidity were performed on the filtrate. The same conditions and procedures were used for commercial ferric compound and the performance of the two solutions was compared.

3.5.3 Effect of time

A volume of 1000 mL of raw aqueous solution was added into six 1000 mL beakers, into which 0.2 mL of the ferric solution was added. The mixtures were agitated at 1, 2, 5, 5, 10, 15, 30 minutes at optimum mixing speed by utilizing a jar test stirrer. Thereafter, the samples were afforded 60 minutes for the suspended solids to settle. The turbidity of the settled water was determined. The supernatant was filtered using Whatman gravity filter. The filtrate was analysed for pH, electrical conductivity, and turbidity. The same conditions and procedures were used for commercial ferric compound and the performance of the two solutions was compared. Optimum conditions obtained from the aforesaid experiments was used to evaluate the performance of the coagulants against the real raw water sample and the real sample from the wastewater that uses ferric chloride for coagulation. This was then used to compare the synthesized coagulant against the commercial coagulant.

3.6 Quality control

The laboratory measurements were subjected to analytical quality control (AQC) and quality assurance (QA) processes. These procedures were conducted in accordance with the standards set by the US National Institute of Standards and Technology (NIST) and the protocols established by the SANAS authorized laboratory. The samples were collected and analyzed using established and recognized methods and procedures, both on-site and off-site, as outlined in the recommendations set by the American Public Health Association (APHA) (Greenberg et al., 2010).

3.7 Validity and reliability or trustworthiness of data

To maintain the reliability, trustworthiness, and validity of the results, experiments were performed in triplicate and results were reported as mean values with the SDV inserted. The SDV that is >10% were nullify the results and experiments were repeated. Also, the samples were analysed in triplicate to ensure validity and reliability or trustworthiness in the present study and this were done in an accredited laboratory using calibrated instruments and facilities.

3.8 Data analysis

Data acquired from this study was processed using Microsoft excel. This aided in determining the significance of the obtained data including regression analysis amongst other statistical analysis that need to be pursued. Specifically, time trend graphs were produced and analysed using Microsoft. Percentage removal to determine efficacy of the feedstock were determined using aforementioned statistical tools. All the data acquired for the use of synthesized Fe(III) as a coagulant were statistically analysed for correlation and simple linear regression using Microsoft excel. Data collection was done using the laboratory information management system (LIMS) and the data captured was verified for correctness. Statistical calculations were done on obtained data to get the mean, minimum, maximum values, and the analysis was done in triplicates by Microsoft Excel. The essence of this was to show the efficacy of the material and removal of contaminants and to determine statistical significance, variation, and disparities.

3.9 Ethical considerations and clearance

This study did not use living organisms as objects of the study. Ethical clearance was obtained from Unisa Research Integrity Office (***2023/CAES_HREC/070***). Consent for sampling AMD was obtained from the mining house authorities. Magalies Water Scientific Services, a SANAS 17025 accredited laboratory was used for the laboratory analysis.

CHAPTER FOUR

RESULTS AND DISCUSSIONS

This chapter presents the results of the experiments carried out to meet the objectives of this study. The results were obtained using the methodologies described in Chapter 3. This section corroborates results from a laboratory study. The used AMDs were collected from the beginning of the experiments and post optimisation studies to check the efficacy of the material, as such, there might be some variations in the water quality of AMD used for optimisation and for the performance verification at optimum conditions.

4.1 Elemental composition of the recovered Fe(III)

The elemental composition of the Fe(III) material, which was selectively recovered from AMD and used for $FeCl_3$ production as characterised using XRF is summarised in **Table 4.1.**

As was expected, Fe(III) was the main constituent, by and large, while other minor impurities, which were initially embedded in AMD, were also identified and they comprised of Al, Mn, and sulphate. Mg and Ca which are from the parent material were also observed to be present in the resultant sludge. Notably high loss of ignition (LoI) was observed, and this could be attributed to water, volatile compounds, and organic substances in the matrices of the recovered Fe-rich sludge.

The LoI denotes the hydrous nature of the recovered material, and it corroborates what has been reported in other studies (Akinwekomi et al., 2020, Masindi et al., 2022a, Nkele et al., 2022). Minor fractions of Ca, S, Mn, and Al were also observed, and this confirms the sinking of metals from AMD to the sludge. Mn and Al are associated to hydroxides, oxy-hydrosulphates, and possible carbonates during the recovery of Fe(III) from mine water, while sulphate may be linked to gypsum and oxy-hydrosulphates.. Other results on the chemical, microstructural, and mineralogical composition has been reported in our previous studies (Masindi et al., 2016, Masindi et al., 2017a, Masindi et al., 2018c, Masindi et al., 2018d, Masindi et al., 2019).

Table 4.1: Elemental composition of the sludge used for the production of ferric chloride coagulant.

Elements	**Standard**		**Real sample**
Wt. %.	**BHV01 Certified**	**BHV01 Analysed**	**Recovered Fe(III)**
SiO_2	**49.94**	49.82	1.96
Al_2O_3	**13.8**	14.26	2.27
MgO	**7.23**	7.82	5.36
Na_2O	**2.26**	1.89	1.28
P_2O_5	**0.273**	0.34	0.11
Fe_2O_3	**12.23**	11.32	65.23
K_2O	**0.52**	0.54	0.42
CaO	**11.4**	10.83	4.72
TiO_2	**2.71**	2.54	0.05
V_2O_5	**0.0566**	0.06	0.01
Cr_2O_3	**0.0422**	0.04	0.01
MnO	**0.168**	0.17	0.10
NiO	**0.0154**	0.01	0.01
CuO	**0.017**	0.02	0.01
ZrO_2	**0.0242**	0.03	0.04
S		0.02	7.02
Co_3O_4		0.01	0.03
ZnO		0.01	0.01
SrO		0.12	0.23
Y_2O_3		0.05	0.01
BaO		-	0.88
LOI		0.07	9.29
TOTAL	**100.69**	**99.98**	**99.01**

Most importantly, the presence of Fe, Al, Mg, Mn, and sulphate will significantly aid in the removal of contaminants in drinking water or municipal wastewater.

4.2 Chemical composition of ferric chloride

Chemical composition of the synthesized and commercial ferric chloride are summarised in **Table 4.2.**

Table 4.2: Chemical composition of the synthesized and commercial ferric chloride.

Elements	Units	Synthesized Fe(III)	Commercial Fe(III)
Fe	mg/L Fe	13700	28000
Mn	mg/L Mn	80	1300
Cr	mg/L Cr	0.01	2.2
Cu	mg/L Cu	0.01	1.1
Ni	mg/L Ni	0.09	0.8
As	mg/L As	0.6	0.4
pH @ 25°C	pH units	2.11	1.8
Al	mg/L Al	470	1001
EC @ 25°C	mS/m	34000	140000
Sulphate	mg/L SO_4	1541	320
Zn	mg/L Zn	0.02	5.8
Ca	mg/L Ca	13	2.4
Mg	mg/L Mg	66	0.66

As was expected, Fe(III) was the main constituent, by and large, while other minor impurities, which were initially embedded in AMD, were also identified and they comprise Al, Mn, and sulphate. Mg and Ca which are from the parent material were also observed to be present in the resultant sludge. The dominance of Mn in the commercial ferric could be attributed to the use of Mn for oxidation of Fe(II) to Fe(III) hence its elevated concentration. Al and sulphate also appear to be amongst the intermediates elements, and this denotes that these are the impurities in the elements that are used for the production of Fe(III). Conductivity is very high due to the amount of chemicals dissolved in the concentrated solution, however, these elements will be significantly low in the Fe(III) used for coagulation since 0.7 mL in a L is used for the production of stock solution (Section 3.3).

4.3 Optimization studies

4.3.1 Effect of ferric chloride dosage on the water treatment

First, the effect of the AMD-synthesized $FeCl_3$ dosage on river water treatment was examined. As mentioned above, L:L ratios in the range 0.1 to 1 mL:L ($FeCl_3$ dosage to river water) were examined and the percentage (%) removals of turbidity, colour, Al, As, Cr, Cu, Fe, Mn, Ni, and Zn were estimated. To provide context and insight the same L:L ratios were also examined when using the commercially available $FeCl_3$. Results are shown in **Figure 4.1**.

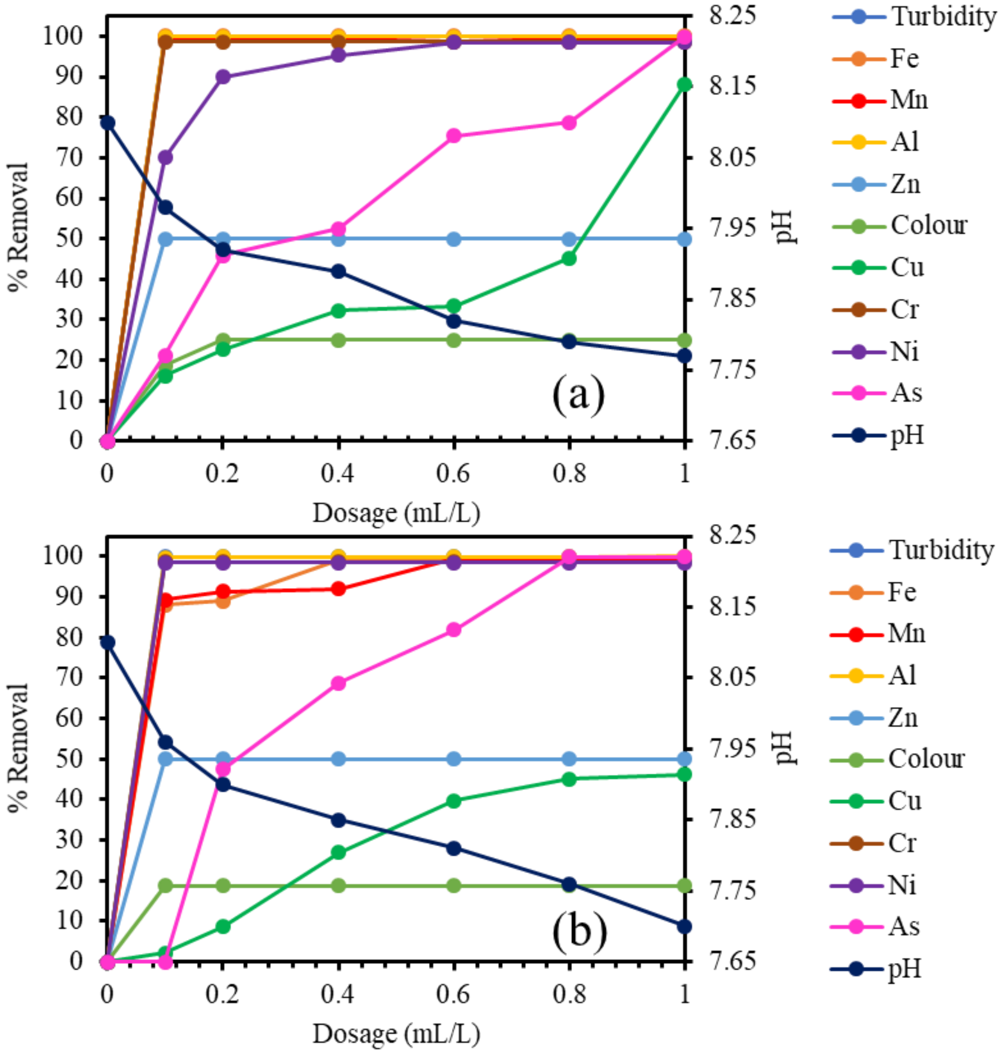

Figure 4.1: Contaminants/indicators percentage removal and pH variations in river water when treated with different dosages of a) AMD-synthesised $FeCl_3$ and b) commercial $FeCl_3$. **(Conditions**: 1 min mixing at 200 rpm, followed by 60 min settling time at ambient temperature and pH).

Regarding the AMD-synthesized $FeCl_3$ (**Figure 4.1a**), it was identified that even at the lower end of the examined range, i.e., 0.1 mL/L, turbidity, Al, Fe, Cr, and Mn was practically removed (≥99% removal). The removal of Zn also plateaued, but the percentage removal was

50%. However, this is not an issue since the initial Zn concentration in the raw river water is many orders of magnitude lower than the ≤ 5 mg/L SANS 241:2015 limit for Zn in drinking water. Colour removal optimizes at the next examined dosage (0.2 mL/L). Again, its percentage removal is only 25%, but this does not affect the results since colour is not an issue even at the raw water. Ni removal optimizes at 0.2 mL/L dosage (98.5% removal) whereas As and Cu removal increase with increasing dosages and is 99.8% and 88.2% at the last examined dosage (1 mL/L), respectively. However, their concentration in the raw river water was below the SANS 241:2015 limit, and therefore, their removal efficiencies cannot be considered a limiting factor when examining the optimum coagulant dosage. As a result, it appears that the first examined dosage (0.1 mL/L) suffices for the removal of the contaminants of concern, i.e., turbidity, Fe, and Al, whereas the next examined dosage (0.2 mL/L) further optimizes the removal of most of the other contaminants. Finally, as was expected the pH of the treated water gradually decreased with increasing $FeCl_3$ dosages, starting from pH 8.1 at the raw drinking water matrix to 7.7 at the last examined dosage (1 mL/L).

Similar results were obtained for the commercially available $FeCl_3$ (**Figure 4.1b**), with the main difference being that Fe is not practically removed at the first examined value, but its removal efficiency increasing with increases dosages. This is also the case for Mn, which percentage removal plateaus at a higher dosage (0.6 mL/L), when compared to the AMD-synthesized $FeCl_3$. On the other hand, Ni removal optimizes at the first examined ranged, but colour achieves a lower removal efficiency. Nonetheless, Fe concentration greatly reduces at the first examined dosage (0.1 mL/L) and its concentration becomes lower than the recommended limit for drinking water, while Mn, Ni, and colour concentrations were below the recommended limit for drinking water and therefore do not affect the results. As such, both the AMD-synthesized and the commercially available $FeCl_3$ have similar performances when used for river water treatment in the South African setting and in both cases the optimal coagulant dosage is 0.2 mL/L.

The higher efficacy of the AMD-synthesized $FeCl_3$ in Fe and Mn removal is likely traced back to the small quantities of Mg and Al, among others, which co-precipitated along with Fe(III) and therefore also find their way in the AMD-synthesized $FeCl_3$. The presence of such cations (Mg and Al) is known to further improve the removal efficiency of Fe and particularly Mn (Jones and Knocke, 2017).

4.3.2 Effect of mixing speed

The effect of mixing speed on the percentage removal of the contaminants/indicators under study is shown in **Figure 4.2**.

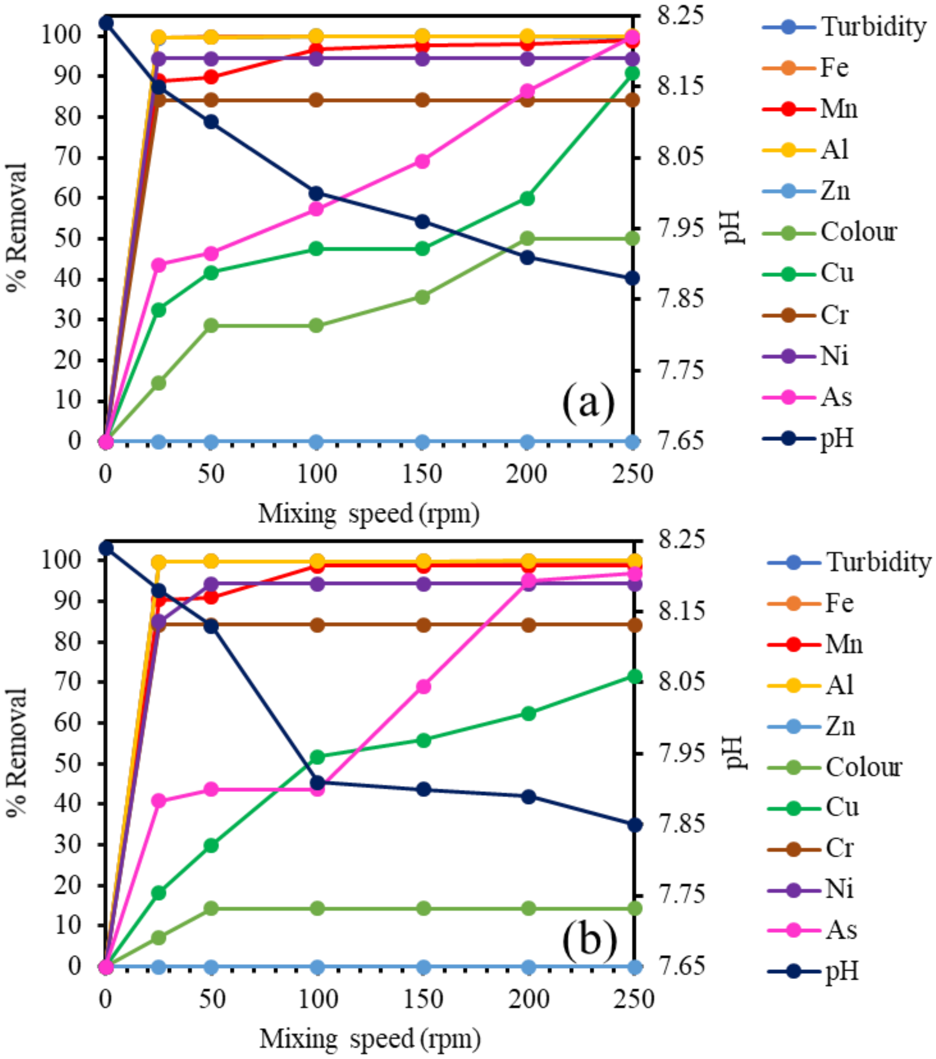

Figure 4.2: Contaminants/indicators percentage removal and pH variations in river water when treated at different mixing speeds for the a) AMD-synthesised $FeCl_3$ and b) commercial $FeCl_3$. **(Conditions**: 0.2 mL/L dosage and 1 min mixing followed by 60 min settling time at ambient temperature and pH).

As mentioned, six different mixing speeds were examined, i.e., 25, 50, 100, 150, 200, and 250 rpm. As shown in **Figure 4.2a**, when using the AMD-synthesized $FeCl_3$, even at the lower end of the examined mixing speed, i.e., 25 rpm, the removal efficiencies for turbidity, Fe, Cr, Ni, and Al are very high (≥99%) and only slightly increase with increasing mixing speeds. Colour removal further increases at the next examined mixing speed, i.e., 50 rpm, and remains stable up to the last examined mixing speed where it slightly increases. This is also the case for Mn removal, which enjoys a steep increase at 25 rpm, then, at the next two mixing speeds, a milder increase is observed and thereafter a slower increase with increasing mixing speed. On the other hand, As and Cu removal appears to increase with increasing mixing speeds and achieve >90% removal at the last examined mixing speed. Finally, as was expected, the pH steadily decreases with increasing mixing speeds, and this suggest the higher distribution and therefore interaction with the contaminants. at higher mixing speeds. Overall, the 100-rpm mixing speed appears to be optimum since mixing is an energy intensive process while at the 100 rpm the water has already been decontaminated and the improved removal of As, Cu, and Mn at higher mixing speed does not add further value since their concentration at 100 rpm are already well below the prescribed limits (SANS 241:2015) for drinking water.

Similar results were obtained when the commercially available $FeCl_3$ coagulant was used to treat the river water. Again, Mn removal was observed to be higher when using the AMD-synthesized $FeCl_3$ for the reasons discussed above.

4.3.3 Effect of contact time

The last examined parameter is the effect of contact time (mixing duration). Specifically, six contact times, i.e., 1, 2.5, 5, 10, 15 and 30 min, were examined and results are shown in **Figure 4.3**.

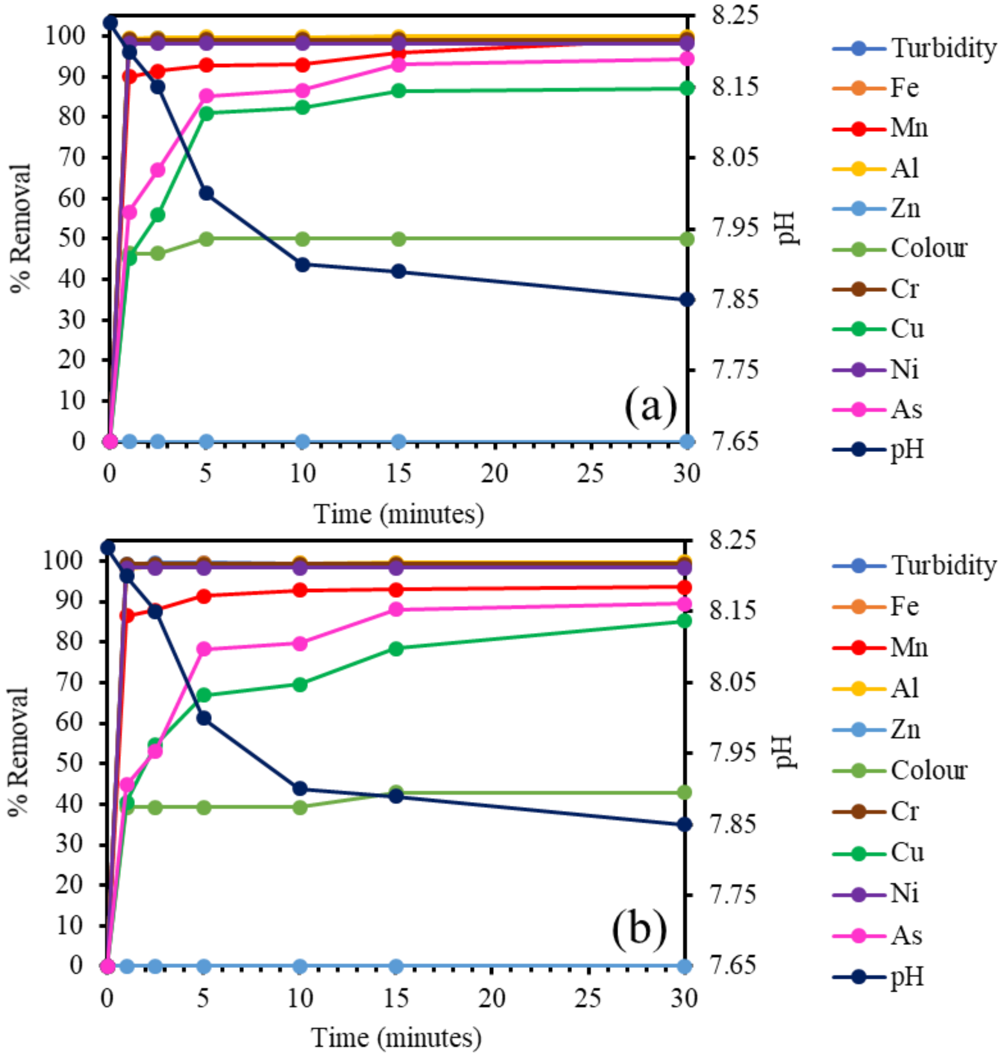

Figure 4.3: Contaminants/indicators percentage removal and pH variations in river water when treated for different contact times for the a) AMD-synthesised $FeCl_3$ and b) commercial $FeCl_3$. (**Conditions**: 0.2 mL/L dosage at 100 rpm mixing speed, followed by 60 min settling time at ambient temperature and pH).

For the AMD-synthesized $FeCl_3$ (**Figure 4.3a**), increasing mixing durations are beneficial for contaminants removals, since the percentage removals for all examined contaminants/indicators increase with increasing mixing durations. In more detail, it was observed that turbidity, Fe, Al, Cr and Ni removal plateaus at the first examined mixing duration (1 min), whereas colour removal was observed to be 46% at first mixing duration and slightly increased to 50% removal plateaus at 5 min mixing duration. For Mn, a high (90%) removal was observed at the first examined mixing duration and thereafter slightly increase with increasing contact time. This is also the case for Cu, where around 45% is removed at the first examined mixing duration and this value doubles (81%) at 5 min contact time and then slowly increases with increasing contact time. The pH also appears to decrease with increasing contact times, and this can be traced back to $FeCl_3$ increasing dissolution with increasing contact times. On the other hand, As removal steeply increases at up to 5 min contact time and then gradually increases until the last examined mixing duration. As was expected, similar results were obtained for the commercial $FeCl_3$ (**Figure 4.3b**). The results are consistent with the ones for coagulant dosage and mixing speed, since the efficiency of the AMD-synthesized $FeCl_3$ in Mn and Fe removal is higher for the reasons discussed above. Overall, in both cases 5 min appears to optimize treatment efficiency, but not at the expense of energy intensity (higher contact times translate to higher mixing durations).

4.4 Efficacy of the AMD-synthesized coagulant for river water and wastewater treatment

After the optimum conditions were identified, i.e., 0.2 mL/L dosage and 5 min mixing at 100 rpm, the efficacy of both the AMD-synthesized and the commercial $FeCl_3$ for the treatment of raw (river) water as well as of wastewater was examined.

4.4.1 River water treatment

The results for the treatment of the real river water, which currently supplies the Cullinan drinking water plant in South Africa was first examined (**Table 4.3**). As shown in **Table 4.3**, the efficacy of the AMD-synthesized coagulant in water treatment is on par, and in many instances even better, than the commercial $FeCl_3$ that is currently employed by the South African drinking water industry. Specifically, for the AMD-synthesized $FeCl_3$ the removal efficacy for Al≥ ammonia≥ turbidity≥ Fe≥ Cr≥ Ni≥ COD≥ Mn≥ Cu≥ nitrite≥ nitrate≥ colour ≥ Ca ≥ alkalinity≥ Mg≥ K≥ Na≥ sulphate≥ EC≥ pH. Similar results were obtained for the commercial $FeCl_3$, with the removal efficacy for the same contaminants/parameters being

Therefore, in both cases, river water was treated to a large extent, but more importantly the values for all examined contaminants/indicators were within the South African National Standard for drinking water, i.e., SANS 241-1:2015 specifications.

Table 4.3: The physicochemical parameters of the raw and the $FeCl_3$ treated river water.

	Units	Raw	Limits	AMD $FeCl_3$	% removal	$FeCl_3$	% removal
Turbidity	NTU	265	≤ 1.0	0.891	99.7	0.981	99.6
pH	-	8.4	≥5.0 to ≤9.7	8.04	4.3	8.0	4.8
EC	mS/m	30	≤ 170	28	6.7	29	3.3
Sulfate	mg/L	31	≤250	28	9.7	29	6.5
Fe	µg/L	600	≤300	3.1	99.5	3.5	99.4
Mn	µg/L	14	≤100	1	92.9	1,2	91.4
Al	µg/L	1120	≤300	2.2	99.8	9.8	99.1
Cr	µg/L	7.8	≤50	0.06	99.2	0.06	99.2
Cu	µg/L	14.8	≤2000	2.8	81.1	4.9	66.9
Ni	µg/L	5.1	≤70	0.09	98.2	0.09	98.2
Alkalinity	mg/L	192	≥250	149	22.4	141	26.6
Zn	mg/L	0.02	≤5.0	0.02	0	0.02	0
Colour	mg/L	28	≤15	14	50.0	17	39.3
Ca	mg/L	41	≤300	21	48.8	22	46.3
Mg	mg/L	17	≤100	15	11.8	15	11.8
Ammonia	mg/L	3.9	≤1.5	0.009	99.8	0.009	99.8
COD	mg/L	213	0.0	10	95.3	12	94.4
Na	mg/L	20	≤200	18	10	19	5.0
K	mg/L	9.9	≤100	8.9	10.1	9	9.0
Nitrate	mg/L	0.25	≤11	0.12	52.0	0.18	28
Nitrite	mg/L	0.037	≤0.9	0.012	67.6	0.028	24.3

Overall, the performance of the AMD synthesized coagulant is on par with, and in some instances even better than the commercial Fe(III). Finally, even though river water and surface water in South Africa is typically heavily polluted (Zachary et al., 2018), the identified $FeCl_3$ dosage suggest that the river water under study is not severely polluted, since, for example, in a case study for canal water treatment in Pakistan the optimum $FeCl_3$ dosage was 13 mg/L (Haydar et al., 2010).

4.4.2 The physicochemical properties of wastewater treatment plant (P1)

The results for the treatment of the real wastewater at optimum conditions, i.e., 5 min contact time and 0.2 mL dosage, 100 rpm are discussed separately. The quality of the wastewater, before and after the treatment with the Fe(III) coagulant, is shown in **Table 4.4**.

Table 4.4: The physicochemical parameters of the raw and treated wastewater at optimum conditions.

	Units	Limits	Raw	Rec $FeCl_3$	% Removal	Com $FeCl_3$	% Removal
Turbidity	NTU	<5	80	1.9	97.6	1.9	97.6
pH	-	5.5-9	8.2	7.92	3.4	7.91	3.5
EC	mS/m	0-700	258	251	2.7	251	2.7
Sulfate	mg/L	0-500	39	36	7.7	37	5.1
Fe	µg/L	0-0.1	245	37	84.9	39	84.1
Mn	µg/L	0-0.05	262	20	92.4	28	89.3
Al	µg/L		120	2.2	98.2	2.9	97.6
Cr	µg/L	0.01	32	2.5	92.2	2.8	91.3
Cu	µg/L	0-1	65	19	70.8	17	73.8
Ni	µg/L	0-0.07	105	12	88.5	12	88.5
Alkalinity	mg/L		749	749	0	749	0
Zn	mg/L	0-0.5	0.04	0.03	25	0.02	50
Colour	mg/L		210	200	4.8	190	9.5
Ca	mg/L	0-32	210	38	81.9	37	82.4
Mg	mg/L	0.30	140	8.8	93.7	8.3	94.1
Ammonia	mg/L	1	25	1.9	92.4	2.1	91.6
COD	mg/L	250	455	68	85.1	69	84.8
Na	mg/L	0-50	84	81	3.6	84	0
K	mg/L	0-50	99	93	6.1	95	4.1
Nitrate	mg/L	15	171	75	56.1	150	12.3
Nitrite	mg/L	15	30	10	66.7	10	66.7

As shown in **Table 4.4**, the interaction of the wastewater with the AMD-synthesized and with the commercial $FeCl_3$ greatly improved its quality. The performance of the recovered Fe(III) is comparable to that of the commercial Fe(III).

4.4.3 The physicochemical properties of wastewater treatment plant (P2)

The results for the treatment of the real wastewater at optimum conditions, i.e., 5 min contact time and 0.2 mL dosage, 100 rpm are discussed separately. The quality of the wastewater, before and after the treatment with the Fe(III) coagulant, is shown in **Table 4.5**.

Table 4.5: The physicochemical parameters of the raw and the Fe(III) treated wastewater at optimum conditions.

	Units	Raw	Rec $FeCl_3$	% removal	Com $FeCl_3$	% removal
Turbidity	NTU	229	1.2	99.5	1.5	99.4
pH	-	8.1	7.75	4.3	7.81	3.6
EC	mS/m	88	82	6.8	83	5.7
Sulphate	mg/L	70	70	0	70	0
Fe	µg/L	276	107	61.2	149	46.0
Mn	µg/L	44	1.1	97.5	1.7	96.1
Al	µg/L	62	1.1	98.2	5.4	91.3
Cr	µg/L	0.06	0.06	0	0.06	0
Cu	µg/L	29	1.4	95.2	12	58.6
Ni	µg/L	10	7.9	21	8.9	11
Alkalinity	mg/L	320	307	4.1	299	6.6
Zn	mg/L	0.02	0.02	0	0.02	0
Colour	mg/L	100	57	43	75	25
Ca	mg/L	39	35	10.3	38	2.6
Mg	mg/L	24	20	16.7	23	4.2
Ammonia	mg/L	39.5	13	67.1	31.8	19.5
COD	mg/L	693	21	97.0	22	96.8
Na	mg/L	103	100	2.9	102	1.0
K	mg/L	18	13	27.8	15	16.7
Nitrate	mg/L	1.8	0.81	55	1.1	38.9
Nitrite	mg/L	0.28	0.14	50	0.21	25

As shown in **Table 4.5**, the interaction of the real wastewater with the commercial Fe(III), and recovered Fe(III) greatly improved the quality of this effluent.. The performance of the recovered Fe(III) is compatible to that of the commercial Fe(III).The recovered Fe(III) is more cost-effective and simpler to synthesis, as it utilizes waste materials and adds value to them. It is independent of the use of virgin material. Its performance exceeds that of commercial Fe(III).

CHAPTER FIVE

CONCLUSIONS AND RECOMMENDATIONS

AMD is amongst the main issues of environmental concern in countries with strong mining industries. As such, research has focused on its sustainable treatment, including its beneficiation The overall aim of this study is to recover Fe(III) from acid mine drainage (AMD), synthesize it to its ferric form and subsequently use it as a coagulant for drinking water treatment. This chapter provides a comprehensive description of the concluding observations and recommendations pertaining to the objectives. The research findings also provide an analysis of the gaps, obstacles, and potential areas for further research.

In pursuit of the main aim of study, the following specific objectives were set:

- To evaluate the physicochemical properties of acid mine drainage from mine and river water from Water treatment plant that is supplied by Wilge river before and after treatment.
- To optimize conditions that are suitable for the recovery of Fe(III) from AMD using MgO i.e., brucite, as a seeding material and its characterization.
- To explore the efficacy of the Fe(III)-based coagulant on the removal of indicator contaminants in drinking water.
- To compare the performance of commercially available ferric compounds and the synthesized Fe(III)-based coagulant on the removal of contaminants, including its compliance to SANS 241 specifications.
- To determine effect that could emanate from using ferric recovered from AMD as a coagulant for drinking water.

5.1 Conclusions

In light of the developed objectives, this study successfully demonstrated the feasibility of recovering Fe(III) from acid mine drainage (AMD) for the production of ferric chloride and its successful application for water and wastewater treatment. Findings from this study denoted 0.2 mL/L (v/v ratio), 100 rpm of mixing speed, and 5 minutes of equilibration time as optimum conditions for commercial and recovered Fe(III). Results were comparable between the commercial ferric and recovered ferric hence demonstrating notable feasibility of replacing commercial Fe(III) with recovered Fe(III). The water quality assessment denoted the concentration of toxic substances to be within SANS 241 specifications hence proving that the materials is chemically stable, and it does not pose any toxicological and hazardous effects. The water sample was analysed for hazardous substances by quantifying the chemical concentration and comparing it to the specified limit outlined in SANS 241. The produced ferric chloride has a chemical composition with low concentrations of components such as Cr < 0.01, Cu ≤ 0.01, As ≤ 0.6, and Zn ≤ 0.08. The absence of harmful substances in the water, as shown by the water quality results after treatment with recovered Fe(III), ensures the safety of the product. As such, findings from this study proved the feasibility of recovering Fe(III) from acid mine drainage and explore its application for the removal of contaminants from water and wastewater matrices. As inspired by the terminal findings, this study will go a long way in fostering the concept of circular economy, waste beneficiation, waste reuse, and waste valorisation specifically when looked under the sustainability paradigm. Based on the findings, insights on iron recovery under the circular economy concept have been noted. In this study, AMD exists as a source of Fe(III). The extraction of Fe(III) from AMD is a significant advancement that will alleviate the demand for new resources. This will significantly reduce the amount of sludge produced during the treatment of AMD and yield a useful chemical coagulant. The findings indicate that it is possible to substitute commercially available Fe(III)-based coagulants with those derived from Fe(III) extracted from AMD. This can lead to chances for implementing sustainable methods of water and wastewater treatment, as well as the implementation of circular economy principles through the process of waste beneficiation and reuse. Future research must put emphasize on the following research gaps; dwell deeper into assessing toxicity of the recovered product and performing life cycle assessment of the product.

5.2 Recommendations

The findings from this study revealed various avenues that need future research to enhance and refine conclusions deduced from this study as follows:

- There is need to assess the effect of cross contamination and cross chemicals recovery, i.e., with Al(III) and Mn(II) or other chemicals, on the efficacy of the synthesized polymer along with toxicological effects. This can be achieved by conducting toxicity testing such as direct toxicity assessment, screening for toxicity compounds in water and/or toxicity identification evaluation.

- Pursue techno-economic analysis of recovering the Fe(III) from acid mine drainage and its use for the production of ferric chloride for drinking water and wastewater treatment with commercially available ferric.
- Assessing the strength of the synthesized ferric chloride in light of the commercially produced chemicals in a quest to determine disparities and competition.
- Demonstrate the feasibility of completing the value chain by employing coupling techniques such as softening and filtration technologies for the reclamation of drinking water or water fit-for-purpose.
- Perform life cycle assessment of the proposed technology and approach in a quest to assess its sustainability and ecological footprints of the process.

REFERENCES

Abdel-Fatah, M. A., Hawash, S. I. & Shaarawy, H. H. 2021. Cost-effective Clean Electrochemical Preparation of Ferric Chloride and its Applications. Egyptian Journal of Chemistry, 64**,** 3841-3851.

Acharya, B. S. & Kharel, G. J. J. O. H. 2020. Acid mine drainage from coal mining in the United States–An overview. 588**,** 125061.

Agboola, O., Mokrani, T., Sadiku, E. R., Kolesnikov, A., Olukunle, O. I., Maree, J. P. J. M. W. & Environment, T. 2017. Characterization of two nanofiltration membranes for the separation of ions from acid mine water. 36**,** 401-408.

Aguiar, A. O., Andrade, L. H., Ricci, B. C., Pires, W. L., Miranda, G. A. & Amaral, M. C. S. 2016. Gold acid mine drainage treatment by membrane separation processes: An evaluation of the main operational conditions. Separation and Purification Technology, 170**,** 360-369.

Akinwekomi, V., Maree, J. P., Masindi, V., Zvinowanda, C., Osman, M. S., Foteinis, S., Mpenyana-Monyatsi, L. & Chatzisymeon, E. 2020. Beneficiation of acid mine drainage (AMD): A viable option for the synthesis of goethite, hematite, magnetite, and gypsum – Gearing towards a circular economy concept. Minerals Engineering, 148**,** 106204.

Akinwekomi, V., Maree, J. P., Zvinowanda, C. & Masindi, V. 2017. Synthesis of magnetite from iron-rich mine water using sodium carbonate. Journal of Environmental Chemical Engineering, 5**,** 2699-2707.

Almeida, V. O. & Schneider, I. a. H. 2020. Production of a ferric chloride coagulant by leaching an iron ore tailing. Minerals Engineering, 156**,** 106511.

Amaral, M. C., Grossi, L. B., Ramos, R. L., Ricci, B. C. & Andrade, L. H. J. D. 2018. Integrated UF–NF–RO route for gold mining effluent treatment: From bench-scale to pilot-scale. 440**,** 111-121.

Ansari, A. A., Shamim, M. A., Khan, A. M., Anwar, K. & Wani, A. A. 2023. Nanomaterials as a cutting edge in the removal of toxic contaminants from water. Materials Chemistry and Physics, 295**,** 127092.

Anyakora, N. V., Ajinomoh, C. S., Ahmed, A. S., Mohammed-Dabo, I. A., Ibrahim, J., Jiniya, B. a. J. W. J. O. E., Pure & Sciences, A. 2012. Sustainable technology-based strategy for processing water works sludge for resource utilization. Environmental Science & Technology, 2**,** 161.

Aslam, T., Masindi, V., Ahmad, A. & Chatzisymeon, E. 2023. Valorization of Acid Mine Drainage into an Iron Catalyst to Initiate the Solar Photo-Fenton Treatment of Municipal Wastewater. Environments, 10.

Bai, S., Bi, Y., Li, J., Yu, P., Ding, Z., Lv, C. & Wen, S. 2021. Innovative utilization of acid mine drainage (AMD): A promising activator for pyrite flotation once depressed in a high alkali solution (HAS)–Gearing towards a cleaner production concept of copper sulfide ore. Minerals Engineering, 170**,** 106997.

Balaram, V. 2019. Rare earth elements: A review of applications, occurrence, exploration, analysis, recycling, and environmental impact. Geoscience Frontiers, 10**,** 1285-1303.

Beltrami, D., Deblonde, G. J.-P., Bélair, S. & Weigel, V. 2015. Recovery of yttrium and lanthanides from sulfate solutions with high concentration of iron and low rare earth content. Hydrometallurgy, 157**,** 356-362.

Besada, H. & Werner, K. 2015. An assessment of the effects of Africa's water crisis on food security and management. International Journal of Water Resources Development, 31**,** 120-133.

Bologo, V., Maree, J. P. & Carlsson, F. 2012. Application of magnesium hydroxide and barium hydroxide for the removal of metals and sulphate from mine water. Water SA, 38**,** 23-28.

Bolto, B. & Gregory, J. 2007. Organic polyelectrolytes in water treatment. Water Research, 41**,** 2301-2324.

Bortnikova, S., Gaskova, O., Yurkevich, N., Saeva, O. & Abrosimova, N. 2020. Chemical Treatment of Highly Toxic Acid Mine Drainage at A Gold Mining Site in Southwestern Siberia, Russia. Minerals, 10**,** 867.

Brandt, M. J., Johnson, K. M., Elphinston, A. J. & Ratnayaka, D. D. 2017. Chapter 8 - Storage, Clarification and Chemical Treatment. In: BRANDT, M. J., JOHNSON, K. M., ELPHINSTON, A. J. & RATNAYAKA, D. D. (eds.) Twort's Water Supply (Seventh Edition). Boston: Butterworth-Heinemann.

Brewster, E. T., Freguia, S., Edraki, M., Berry, L. & Ledezma, P. 2020. Staged electrochemical treatment guided by modelling allows for targeted recovery of metals and rare earth elements from acid mine drainage. Journal of Environmental Management, 275**,** 111266.

Bromfield, T. C. & Vosloo, A. C. Recent advances in the development of Fischer-Tropsch catalysts at sasol. Macromolecular Symposia, 2003. Wiley Online Library, 29-34.

Buzzi, D. C., Viegas, L. S., Rodrigues, M. a. S., Bernardes, A. M. & Tenório, J. a. S. 2013. Water recovery from acid mine drainage by electrodialysis. Minerals Engineering, 40**,** 82-89.

Cánovas, C. R., Macías, F. & Pérez-López, R. 2016. Metal and acidity fluxes controlled by precipitation/dissolution cycles of sulfate salts in an anthropogenic mine aquifer. Journal of Contaminant Hydrology, 188**,** 29-43.

Chávez, G. 2017. Recovery of rare earth elements from acid mine waters by using phosphate based precipitation processes. Escola Tècnica Superior d'Enginyeria Industrial de Barcelona**,** 1-8.

Chen, G., Ye, Y., Yao, N., Hu, N., Zhang, J. & Huang, Y. 2021. A critical review of prevention, treatment, reuse, and resource recovery from acid mine drainage. Journal of Cleaner Production, 329**,** 129666.

Cheong, Y. W., Yim, G.-J., Ji, S. W., Kang, S. S., Skousen, J. J. E. M. & Assessment 2012. Water quality changes of a closed underground coal mine in Korea. 184**,** 503-513.

Churchman, G. J. 2002. Formation of complexes between bentonite and different cationic polyelectrolytes and their use as sorbents for non-ionic and anionic pollutants. Applied Clay Science, 21**,** 177-189.

Cravotta Iii, C. A. 2008. Dissolved metals and associated constituents in abandoned coal-mine discharges, Pennsylvania, USA. Part 1: Constituent quantities and correlations. Applied Geochemistry, 23**,** 166-202.

Craw, D., Rufaut, C. & Pillai, D. 2023. Evolution of Alkaline Mine Drainage and Unique Biodiversity on Soil-Free Mine Substrates, Southern New Zealand. Mine Water and the Environment, 42**,** 3-23.

Craw, D., Rufaut, C. G., Haffert, L. & Todd, A. 2006. Mobilisation and attenuation of boron during coal mine rehabilitation, Wangaloa, New Zealand. The Science of the total environment, 368**,** 444-55.

Cross, K. M., Lu, Y., Zheng, T., Zhan, J., Mcpherson, G. L. & John, V. T. 2014. Chapter 27 - Water Decontamination Using Iron and Iron Oxide Nanoparticles. In: STREET, A., SUSTICH, R., DUNCAN, J. & SAVAGE, N. (eds.) Nanotechnology Applications for Clean Water (Second Edition). Oxford: William Andrew Publishing.

Du Plessis, P. & Maree, J. P. 1994. Neutralisation of acid water in the chemical industry with limestone. Water Science and Technology, 29**,** 93-104.

Felipe, E. C. B., Batista, K. A. & Ladeira, A. C. Q. 2021. Recovery of rare earth elements from acid mine drainage by ion exchange. Environmental Technology, 42**,** 2721-2732.

Fernandes, H. M., Franklin, M. R. & Veiga, L. H. J. W. M. 1998. Acid rock drainage and radiological environmental impacts. A study case of the Uranium mining and milling facilities at Poços de Caldas. 18**,** 169-181.

Flores, R. G., Andersen, S. L., Maia, L. K., José, H. J. & Moreira Rde, F. 2012. Recovery of iron oxides from acid mine drainage and their application as adsorbent or catalyst. J Environ Manage, 111**,** 53-60.

Galhardi, J. A., Bonotto, D. M. J. W., Air, & Pollution, S. 2017. Radionuclides (222Rn, 226Ra, 234U, and 238U) Release in Natural Waters Affected by Coal Mining Activities in Southern Brazil. 228**,** 1-19.

Geldenhuys, A. J., Maree, J. P., De Beer, M. & Hlabela, P. 2003. An integrated limestone/lime process for partial sulphate removal. Journal of the South African Institute of Mining and Metallurgy, 103**,** 345-354.

Goodman, A. J., Bednar, A. J. & Ranville, J. F. 2023. Rare earth element recovery in hard-rock acid mine drainage and mine waste: A case study in Idaho Springs, Colorado. Applied Geochemistry, 150**,** 105584.

Guo, Z. H., Jiang, Z. C., Liu, Y. N. & Wang, S. 2014. Coagulation and sedimentation treating wastewater from W containing multi-metal ore dressing process. Zhongguo Youse Jinshu Xuebao/Chinese Journal of Nonferrous Metals, 24**,** 2393-2399.

Haydar, S., Ahmad, H. & Aziz, J. 2010. Optimization of coagulation-flocculation in the treatment of canal water. Environmental Engineering and Management Journal, 9**,** 1563-1570.

Herlitschke, M., Disch, S., Sergueev, I., Schlage, K., Wetterskog, E., Bergström, L. & Hermann, R. P. 2016. Spin disorder in maghemite nanoparticles investigated using polarized neutrons and nuclear resonant scattering. Journal of Physics: Conference Series, 711**,** 012002.

Hermassi, M., Granados, M., Valderrama, C., Ayora, C. & Cortina, J. L. 2022a. Recovery of rare earth elements from acidic mine waters: An unknown secondary resource. Science of The Total Environment, 810**,** 152258.

Hermassi, M., Granados, M., Valderrama, C., Ayora, C. & Cortina, J. L. J. S. O. T. T. E. 2022b. Recovery of rare earth elements from acidic mine waters: An unknown secondary resource. 810**,** 152258.

Heviankova, S., Špakovská, B., Klimko, T., Kyncl, M., Bilska, Z., Kučerová, L. J. C. J. O. E. & Sciences, E. 2014. Acid mine drainage treatment by ash from wooden chip combustion: study of mine water composition in dependence on the ash dose and duration of mutual interaction. 9**,** 159-170.

Hu, X., Yang, H., Tan, K., Hou, S., Cai, J., Yuan, X., Lan, Q., Cao, J. & Yan, S. 2022. Treatment and recovery of iron from acid mine drainage: a pilot-scale study. Journal of Environmental Chemical Engineering, 10**,** 106974.

Huang, A., Zhi, D., Tang, H., Jiang, L., Luo, S. & Zhou, Y. 2020. Effect of Fe2+, Mn2+ catalysts on the performance of electro-Fenton degradation of antibiotic ciprofloxacin, and expanding the utilizing of acid mine drainage. Science of The Total Environment, 720**,** 137560.

Jones, A. & Knocke, W. R. 2017. Evaluating the role of soluble aluminum in manganese removal via MnOx(s)-coated filtration media in drinking water treatment. Water Research, 111**,** 59-65.

Kamunda, C., Mathuthu, M. & Madhuku, M. 2016. An Assessment of Radiological Hazards from Gold Mine Tailings in the Province of Gauteng in South Africa. Int J Environ Res Public Health, 13.

Kefeni, K. K., Msagati, T. a. M. & Mamba, B. B. 2017. Acid mine drainage: Prevention, treatment options, and resource recovery: A review. Journal of Cleaner Production, 151**,** 475-493.

Kesieme, U. K., Milne, N., Aral, H., Cheng, C. Y. & Duke, M. Novel application of membrane distillation for acid and water recovery from mining waste waters. International mine water association symposium, 2012. 623-630.

Khudaykulova, M., Yuanqiong, H. & Khudaykulov, A. 2022. Economic consequences and implications of the Ukraine-russia war. International Journal of Management Science and Business Administration, 8**,** 44-52.

Kirby, C. & Cravotta, C. 2005. Net alkalinity and net acidity 2: Practical considerations. Applied Geochemistry, 20**,** 1941-1964.

Knuuttila, P., Torpparin, Jokinen, S., Sorsatie, Judin, V.-P., Orvokintie, Ivuorisalo, J., Tasatie, Salanne, S. & Salmelantie. 1994. production of ferric chloride.

Lappas, A. A., Kalogiannis, K. G., Iliopoulou, E. F., Triantafyllidis, K. S. & Stefanidis, S. D. 2016. Catalytic pyrolysis of biomass for transportation fuels. Advances in Bioenergy: The Sustainability Challenge**,** 45-56.

Le, V. G., Vo, T. D. H., Nguyen, B. S., Vu, C. T., Shih, Y. J. & Huang, Y. H. 2020. Recovery of iron(II) and aluminum(III) from acid mine drainage by sequential selective precipitation and fluidized bed homogeneous crystallization (FBHC). Journal of the Taiwan Institute of Chemical Engineers, 115**,** 135-143.

Lefèvre, M. & Dodelet, J.-P. 2003. Fe-based catalysts for the reduction of oxygen in polymer electrolyte membrane fuel cell conditions: determination of the amount of peroxide released during electroreduction and its influence on the stability of the catalysts. Electrochimica Acta, 48**,** 2749-2760.

Li, M., Liu, J., Xu, Y. & Qian, G. 2016. Phosphate adsorption on metal oxides and metal hydroxides: A comparative review. Environmental Reviews, 24**,** 319-332.

Li, Q., Ji, B., Honaker, R., Noble, A., Zhang, W. J. C., Physicochemical, S. A. & Aspects, E. 2022. Partitioning behavior and mechanisms of rare earth elements during precipitation in acid mine drainage. Colloids and Surfaces A: Physicochemical and Engineering Aspects, 641**,** 128563.

Li, R., Li, Q., Gao, S. & Shang, J. K. J. C. E. J. 2012. Exceptional arsenic adsorption performance of hydrous cerium oxide nanoparticles: Part A. Adsorption capacity and mechanism. 185**,** 127-135.

Lopes, F. A., Menezes, J. & Schneider, I. J. I., Aachen, Germany 2011. Acid mine drainage as source of iron for the treatment of sewage by coagulation and Fenton's reaction. international Mine Water Association.

Luptáková, A., Andráš, P. J. W. R. I. S. P. I. A. & Development 2019. Formation of acid mine drainage in sulphide ore deposits. Water Resources, 69**,** 259-276.

Ma, Y., Stopić, S., Xakalashe, B., Friedrich, B., Mwewa, B., Simate, G. S. & Ndlovu, S. 2018a. Hydrometallurgical treatment of acid mine drainage (AMD) solution, International Society of Electrochemistry.

Ma, Y., Stopić, S., Xakalashe, B., Friedrich, B., Mwewa, B., Simate, G. S. & Ndlovu, S. 2018b. Hydrometallurgical treatment of acid mine drainage (AMD) solution.

Macingova, E. & Luptakova, A. 2012. Recovery of Metals from Acid Mine Drainage. Chem. Eng. Trans., 28**,** 109.

Maree, J. P. & Du Plessis, P. 1993. Neutralization of acid mine water calcium carbonate. Proc. IAWQ Conference on Pre-treatment of IndustrialWastewaters, Athens.

Martí-Calatayud, M. C., Buzzi, D. C., García-Gabaldón, M., Ortega, E., Bernardes, A. M., Tenório, J. a. S. & Pérez-Herranz, V. 2014. Sulfuric acid recovery from acid mine drainage by means of electrodialysis. Desalination, 343**,** 120-127.

Masindi, V. 2017a. Recovery of drinking water and valuable minerals from acid mine drainage using an integration of magnesite, lime, soda ash, CO2 and reverse osmosis treatment processes. Journal of Environmental Chemical Engineering, 5**,** 3136-3142.

Masindi, V. 2017b. Recovery of drinking water and valuable minerals from acid mine drainage using an integration of magnesite, lime, soda ash, CO(sub)2 and reverse osmosis treatment processes.

Masindi, V., Akinwekomi, V., Maree, J. P. & Muedi, K. L. 2017a. Comparison of mine water neutralisation efficiencies of different alkaline generating agents. Journal of Environmental Chemical Engineering, 5**,** 3903-3913.

Masindi, V., Chatzisymeon, E., Kortidis, I. & Foteinis, S. 2018a. Assessing the sustainability of acid mine drainage (AMD) treatment in South Africa. Science of The Total Environment, 635**,** 793-802.

Masindi, V. & Foteinis, S. 2021. Recovery of phosphate from real municipal wastewater and its application for the production of phosphoric acid. Journal of Environmental Chemical Engineering, 9**,** 106625.

Masindi, V., Foteinis, S. & Chatzisymeon, E. 2022a. Co-treatment of acid mine drainage and municipal wastewater effluents: Emphasis on the fate and partitioning of chemical contaminants. Journal of Hazardous Materials, 421**,** 126677.

Masindi, V., Foteinis, S., Renforth, P., Ndiritu, J., Maree, J. P., Tekere, M. & Chatzisymeon, E. 2022b. Challenges and avenues for acid mine drainage treatment, beneficiation, and valorisation in circular economy: A review. Ecological Engineering, 183**,** 106740.

Masindi, V., Gitari, M. W., Tutu, H. & De Beer, M. 2015a. Passive remediation of acid mine drainage using cryptocrystalline magnesite: A batch experimental and geochemical modelling approach. Water SA, 41**,** 677-682.

Masindi, V., Gitari, M. W., Tutu, H. & De Beer, M. 2016. Fate of inorganic contaminants post treatment of acid mine drainage by cryptocrystalline magnesite: Complimenting experimental results with a geochemical model. Journal of Environmental Chemical Engineering, 4**,** 4846-4856.

Masindi, V., Gitari, M. W., Tutu, H. & Debeer, M. 2015b. Efficiency of ball milled South African bentonite clay for remediation of acid mine drainage. Journal of Water Process Engineering, 8**,** 227-240.

Masindi, V., Madzivire, G. & Tekere, M. 2018b. Reclamation of water and the synthesis of gypsum and limestone from acid mine drainage treatment process using a combination of pre-treated magnesite nanosheets, lime, and CO2 bubbling. Water Resources and Industry, 20**,** 1-14.

Masindi, V., Ndiritu, J. G. & Maree, J. P. 2018c. Fractional and step-wise recovery of chemical species from acid mine drainage using calcined cryptocrystalline magnesite nano-sheets: An experimental and geochemical modelling approach. Journal of Environmental Chemical Engineering, 6**,** 1634-1650.

Masindi, V., Osman, M. S. & Abu-Mahfouz, A. M. 2017b. Integrated treatment of acid mine drainage using BOF slag, lime/soda ash and reverse osmosis (RO): Implication for the production of drinking water. Desalination, 424**,** 45-52.

Masindi, V., Osman, M. S., Mbhele, R. N. & Rikhotso, R. 2018d. Fate of pollutants post treatment of acid mine drainage with basic oxygen furnace slag: Validation of experimental results with a geochemical model. Journal of Cleaner Production, 172**,** 2899-2909.

Masindi, V., Osman, M. S. & Shingwenyana, R. 2019. Valorization of acid mine drainage (AMD): A simplified approach to reclaim drinking water and synthesize valuable minerals – Pilot study. Journal of Environmental Chemical Engineering, 7**,** 103082.

Masindi, V. & Tekere, M. 2020. Innovative Routes for Acid Mine Drainage (AMD) Valorization. Recovery of Byproducts from Acid Mine Drainage Treatment.

Masindi, V. J. J. O. E. C. E. 2017c. Recovery of drinking water and valuable minerals from acid mine drainage using an integration of magnesite, lime, soda ash, CO2 and reverse osmosis treatment processes. 5**,** 3136-3142.

Mavhungu, A., Foteinis, S., Mbaya, R., Masindi, V., Kortidis, I., Mpenyana-Monyatsi, L. & Chatzisymeon, E. 2020a. Environmental sustainability of municipal wastewater treatment through struvite precipitation: Influence of operational parameters. Journal of Cleaner Production**,** 124856.

Mavhungu, A., Masindi, V., Foteinis, S., Mbaya, R., Tekere, M., Kortidis, I. & Chatzisymeon, E. 2020b. Advocating circular economy in wastewater treatment: Struvite formation and drinking water reclamation from real municipal effluents. Journal of Environmental Chemical Engineering**,** 103957.

Menezes, J., Silva, R., Arce, I. & Schneider, I. 2009a. Production of a poly-ferric sulphate chemical coagulant by selective precipitation of iron from acidic coal mine drainage. Mine Water and the Environment, 28**,** 311.

Menezes, J., Silva, R., Arce, I. & Schneider, I. J. M. E. 2010. Production of a poly-alumino-iron sulphate coagulant by chemical precipitation of a coal mining acid drainage. 23**,** 249-251.

Menezes, J. C. S. S., Silva, R. A., Arce, I. S. & Schneider, I. a. H. 2009b. Production of a Poly-ferric Sulphate Chemical Coagulant by Selective Precipitation of Iron from Acidic Coal Mine Drainage. Mine Water and the Environment, 28**,** 311-314.

Merten, D., Geletneky, J., Bergmann, H., Haferburg, G., Kothe, E. & Büchel, G. 2005. Rare earth element patterns: A tool for understanding processes in remediation of acid mine drainage. Chemie der Erde - Geochemistry, 65, Supplement 1**,** 97-114.

Mohan, D. & Pittman, C. U. 2007. Arsenic removal from water/wastewater using adsorbents—A critical review. Journal of Hazardous materials, 142**,** 1-53.

Moraes, M. L. B., Murciego, A., Álvarez-Ayuso, E. & Ladeira, A. C. Q. J. a. G. 2020. The role of Al13-polymers in the recovery of rare earth elements from acid mine drainage through pH neutralization. Applied Geochemistry, 113**,** 104466.

Moshupya, P., Abiye, T., Mouri, H., Levin, M., Strauss, M. & Strydom, R. 2019. Assessment of Radon Concentration and Impact on Human Health in a Region Dominated by Abandoned Gold Mine Tailings Dams: A Case from the West Rand Region, South Africa. 9**,** 466.

Muedi, K., Masindi, V., Maree, J. P., Haneklaus, N. & Brink, H. 2022. Effective Adsorption of Congo Red from Aqueous Solution Using Fe/Al Di-Metal Nanostructured Composite Synthesised from Fe(III) and Al(III) Recovered from Real Acid Mine Drainage. Nanomaterials.

Mulopo, J. 2016. Direct elemental sulphur recovery from gold acid mine drainage streams. Journal of Environmental Chemical Engineering, 4**,** 4670-4679.

Mwewa, B., Stopić, S., Ndlovu, S., Simate, G. S., Xakalashe, B. & Friedrich, B. 2019a. Synthesis of Poly-Alumino-Ferric Sulphate Coagulant from Acid Mine Drainage by Precipitation. Metals, 9**,** 1166.

Mwewa, B., Stopić, S., Ndlovu, S., Simate, G. S., Xakalashe, B. & Friedrich, B. 2019b. Synthesis of Poly-Alumino-Ferric Sulphate Coagulant from Acid Mine Drainage by Precipitation. 9**,** 1166.

Mwewa, B., Tadie, M., Ndlovu, S., Simate, G. S. & Matinde, E. 2022a. Recovery of rare earth elements from acid mine drainage: A review of the extraction methods. Journal of Environmental Chemical Engineering, 10**,** 107704.

Mwewa, B., Tadie, M., Ndlovu, S., Simate, G. S. & Matinde, E. 2022b. Recovery of Rare Earth Elements from Acid Mine Drainage: A Review of the Extraction Methods. Journal of Environmental Chemical Engineering, 107704.

Naidu, G., Ryu, S., Thiruvenkatachari, R., Choi, Y., Jeong, S. & Vigneswaran, S. 2019. A critical review on remediation, reuse, and resource recovery from acid mine drainage. Environmental Pollution, 247, 1110-1124.

Nkele, K. M., Mpenyana-Monyatsi, L. & Masindi, V. 2022. Fabrication of highly reactive MgO-NPs-CaO-hydrous nanocomposite and its application for the removal of manganese from aqueous solution. Advances in Environmental Technology, 8, 293-309.

Nleya, Y., Simate, G. S. & Ndlovu, S. 2016. Sustainability assessment of the recovery and utilisation of acid from acid mine drainage. Journal of Cleaner Production, 113, 17-27.

Nogueira, E. W., Gouvêa De Godoi, L. A., Marques Yabuki, L. N., Brucha, G. & Zamariolli Damianovic, M. H. R. 2021. Sulfate and metal removal from acid mine drainage using sugarcane vinasse as electron donor: Performance and microbial community of the down-flow structured-bed bioreactor. Bioresource Technology, 330, 124968.

Ntuli, F., Falayi, T. & Thwanane, U. J. W. T. E. E. 2016a. Removal of sulphates from acid mine drainage using desilicated fly ash slag. Waste Management and The Environment, 202, 383-390.

Ntuli, F., Falayi, T. & Thwanane, U. J. W. T. E. E. 2016b. Removal of sulphates from acid mine drainage using desilicated fly ash slag. 202, 383-390.

Oh, C., Han, Y.-S., Park, J. H., Bok, S., Cheong, Y., Yim, G. & Ji, S. 2016. Field application of selective precipitation for recovering Cu and Zn in drainage discharged from an operating mine. Science of the Total Environment, 557–558, 212-220.

Olah, G. A. & Molnár, Á. 2003. Hydrocarbon chemistry, John Wiley & Sons.

Pereira, W. V. D. S., Ramos, S. J., Melo, L. C. A., Dias, Y. N., Martins, G. C., Ferreira, L. C. G. & Fernandes, A. R. 2023. Human and environmental exposure to rare earth elements in gold mining areas in the northeastern Amazon. Chemosphere, 340, 139824.

Pino, L., Beltran, E., Schwarz, A., Ruiz, M. C. & Borquez, R. 2020. Optimization of nanofiltration for treatment of acid mine drainage and copper recovery by solvent extraction. Hydrometallurgy, 195, 105361.

Pratinthong, N., Sangchan, S., Chimupala, Y. & Kijjanapanich, P. 2021. Sulfate removal from lignite coal mine drainage in Thailand using ettringite precipitation. Chemosphere, 285, 131357.

Preub, V., Riedel, C., Koch, T., Thurmer, K. & Domańska, M. J. a. C. E. E. 2012a. Nanofiltration as an effective tool of reducing sulphate concentration in mine water. 3**,** 127-132.

Preub, V., Riedel, C., Koch, T., Thurmer, K. & Domańska, M. J. a. C. E. E. 2012b. Nanofiltration as an effective tool of reducing sulphate concentration in mine water. Architecture Civil Engineering Environment, 3**,** 127-132.

Qureshi, A. 2020. Challenges and Prospects of Using Treated Wastewater to Manage Water Scarcity Crises in the Gulf Cooperation Council (GCC) Countries. Water, 12.

Rao, S. R., Gehr, R., Riendeau, M., Lu, D. & Finch, J. A. 1992. Acid mine drainage as a coagulant. Minerals Engineering, 5**,** 1011-1020.

Rodríguez-Galán, M., Baena-Moreno, F. M., Vázquez, S., Arroyo-Torralvo, F., Vilches, L. F. & Zhang, Z. 2019. Remediation of acid mine drainage. Environmental Chemistry Letters, 17**,** 1529-1538.

Royer-Lavallée, A., Neculita, C. M. & Coudert, L. 2020. Removal and potential recovery of rare earth elements from mine water. Journal of Industrial and Engineering Chemistry, 89**,** 47-57.

Ryan, M. J., Kney, A. D. & Carley, T. L. 2017. A study of selective precipitation techniques used to recover refined iron oxide pigments for the production of paint from a synthetic acid mine drainage solution. Applied Geochemistry, 79**,** 27-35.

Saeid, A. & Chojnacka, K. 2014. Sulfuric Acid. In: WEXLER, P. (ed.) Encyclopedia of Toxicology (Third Edition). Oxford: Academic Press.

Sahinkaya, E., Gungor, M., Bayrakdar, A., Yucesoy, Z. & Uyanik, S. J. J. O. H. M. 2009. Separate recovery of copper and zinc from acid mine drainage using biogenic sulfide. Journal of Hazardous Materials, 171**,** 901-906.

Sahoo, P., Tripathy, S., Equeenuddin, S. M. & Panigrahi, M. 2012. Geochemical characteristics of coal mine discharge vis-à-vis behavior of rare earth elements at Jaintia Hills coalfield, northeastern India. Journal of Geochemical Exploration, 112**,** 235-243.

Salama, E. S., Kim, J. R., Ji, M. K., Cho, D. W., Abou-Shanab, R. a. I., Kabra, A. N. & Jeon, B. H. 2015. Application of acid mine drainage for coagulation/flocculation of microalgal biomass. Bioresour Technol, 186**,** 232-237.

Seo, E. Y., Cheong, Y. W., Yim, G. J., Min, K. W. & Geroni, J. N. 2017. Recovery of Fe, Al and Mn in acid coal mine drainage by sequential selective precipitation with control of pH. CATENA, 148, Part 1**,** 11-16.

Silva, A. M., Cunha, E. C., Silva, F. D. R. & Leão, V. A. 2012a. Treatment of high-manganese mine water with limestone and sodium carbonate. Journal of Cleaner Production, 29–30**,** 11-19.

Silva, R. D. A., Castro, C. D., Vigânico, E. M., Petter, C. O. & Schneider, I. a. H. 2012b. Selective precipitation/UV production of magnetite particles obtained from the iron recovered from acid mine drainage. Minerals Engineering, 29**,** 22-27.

Simate, G. S. & Ndlovu, S. 2014. Acid mine drainage: Challenges and opportunities. Journal of Environmental Chemical Engineering, 2**,** 1785-1803.

Smołka-Danielowska, D. & Walencik-Łata, A. J. M. 2021. The occurrence of selected radionuclides and rare earth elements in waste at the mine heap from the Polish Mining Group. 11**,** 504.

Stilwell, L., Minnitt, R., Monson, T. & Kuhn, G. 2000. An input–output analysis of the impact of mining on the South African economy. Resources policy, 26**,** 17-30.

Sun, M., Ru, X.-R. & Zhai, L.-F. J. a. C. B. E. 2015. In-situ fabrication of supported iron oxides from synthetic acid mine drainage: high catalytic activities and good stabilities towards electro-Fenton reaction. Applied Catalysis B: Environmental, 165**,** 103-110.

Sun, Y.-M., Zhai, L.-F., Duan, M.-F. & Sun, M. 2018. In Situ Fabrication of Electro-Fenton Catalyst from Fe2+ in Acid Mine Drainage: Influence of Coexisting Metal Cations. ACS Sustainable Chemistry & Engineering, 6**,** 14154-14161.

Tabak, H. H., Scharp, R., Burckle, J., Kawahara, F. K. & Govind, R. 2003. Advances in biotreatment of acid mine drainage and biorecovery of metals: 1. Metal precipitation for recovery and recycle. Biodegradation, 14**,** 423-436.

Taghizadeh, A., Taghizadeh, M., Jouyandeh, M., Yazdi, M. K., Zarrintaj, P., Saeb, M. R., Lima, E. C. & Gupta, V. K. 2020. Conductive polymers in water treatment: A review. Journal of Molecular Liquids, 312**,** 113447.

Tetteh, E. K., Rathilal, S., Chetty, M., Armah, E. K. & Asante-Sackey, D. 2019. Treatment of water and wastewater for reuse and energy generation-emerging technologies. Water and wastewater treatment**,** 53-80.

Tzoupanos, N. & Zouboulis, I. Coagulation-flocculation processes in water/wastewater treatment: the application of new generation of chemical reagents. 6th IASME/WSEAS international conference on heat transfer, thermal engineering and environment (HTE'08), August 20th–22nd, Rhodes, Greece, 2008. 309-317.

Vadapalli, V. R. K., Klink, M. J., Etchebers, O., Petrik, L. F., Gitari, W., White, R. A., Key, D. & Iwuoha, E. 2008. Neutralization of acid mine drainage using fly ash, and strength development of the resulting solid residues. South African Journal of Science, 104**,** 317-322.

Vaziri Hassas, B., Rezaee, M. & Pisupati, S. V. 2020. Precipitation of rare earth elements from acid mine drainage by CO2 mineralization process. Chemical Engineering Journal, 399**,** 125716.

Venter, R. & Boylett, M. The evaluation of various oxidants used in acid leaching of uranium. Hydrometallurgy Conference, 2009. Citeseer, 445-456.

Verma, S., Daverey, A. & Sharma, A. 2017. Slow sand filtration for water and wastewater treatment – a review. Environmental Technology Reviews, 6**,** 47-58.

Wagenfeld, J.-G., Al-Ali, K., Almheiri, S., Slavens, A. F. & Calvet, N. 2019. Sustainable applications utilizing sulfur, a by-product from oil and gas industry: A state-of-the-art review. Waste Management, 95**,** 78-89.

Wang, Y., Wang, J., Li, Z., Wang, H., He, X. & Wang, C. J. C. 2021. A novel method based on membrane distillation for treating acid mine drainage: Recovery of water and utilization of iron. Chemosphere, 279**,** 130605.

Wei, X., Viadero Jr, R. C. & Buzby, K. M. 2005. Recovery of iron and aluminum from acid mine drainage by selective precipitation. Environmental engineering science, 22**,** 745-755.

Wen, B., Yuan, D.-A., Shan, X.-Q., Li, F.-L., Zhang, S.-Z. J. E. P. & Bioavailability 2001a. The influence of rare earth element fertilizer application on the distribution and bioaccumulation of rare earth elements in plants under field conditions. 13**,** 39.

Wen, B., Yuan, D.-A., Shan, X.-Q., Li, F.-L., Zhang, S.-Z. J. E. P. & Bioavailability 2001b. The influence of rare earth element fertilizer application on the distribution and bioaccumulation of rare earth elements in plants under field conditions. Chemical Speciation & Bioavailability, 13**,** 39.

Wysocka, M., Chałupnik, S., Chmielewska, I., Janson, E., Radziejowski, W. & Samolej, K. 2019. Natural Radioactivity in Polish Coal Mines: An Attempt to Assess the Trend of Radium Release into the Environment. Mine Water and the Environment, 38**,** 581-589.

Xia, S., Song, Z., Zhao, X. & Li, J. J. J. O. W. P. E. 2023a. Review of the recent advances in the prevention, treatment, and resource recovery of acid mine wastewater discharged in coal mines. Journal of Water Process Engineering, 52**,** 103555.

Xia, S., Song, Z., Zhao, X. & Li, J. J. J. O. W. P. E. 2023b. Review of the recent advances in the prevention, treatment, and resource recovery of acid mine wastewater discharged in coal mines. 52**,** 103555.

Xu, X., Zhu, W., Wang, Z., Witkamp, G.-J. J. P. & Soil 2003a. Accumulation of rare earth elements in maize plants (Zea mays L.) after application of mixtures of rare earth elements and lanthanum. Plant and Soil, 252**,** 267-277.

Xu, X., Zhu, W., Wang, Z., Witkamp, G.-J. J. P. & Soil 2003b. Accumulation of rare earth elements in maize plants (Zea mays L.) after application of mixtures of rare earth elements and lanthanum. 252**,** 267-277.

Yang, B., Jiang, S., Zhang, C., Zhao, G., Wu, M., Xiao, N. & Su, P. J. C. 2021. Recovery of iron from iron-rich pickling sludge for preparing P-doped polyferric chloride coagulant. Chemosphere, 283**,** 131216.

Yuan, M., Chen, K. & Qiu, G. J. M. U. O. M. R. 2000. Study on Process for Preparation of Active Manganese Dioxide from Natural Manganese Ore.(3) Oxidation and Recovery of Manganese (II) Ion in Leaching Solution. Minerals Engineering, 1**,** 16-18.

Yuan, S., Xiao, H., Wang, R., Li, Y. & Gao, P. 2022. Improved iron recovery from low-grade iron ore by efficient suspension magnetization roasting and magnetic separation. Minerals Engineering, 186**,** 107761.

Zachary, D., Courtney, C. & Steve, H. 2018. A delicate balance: Water scarcity in South Africa. In: 13, S. A. R. (ed.).

Zafra, M., Alarcón-Hincapié, J. & Gutiérrez-Malaxechebarría, A.-M. 2020. Cost/Benefit Analysis for the Use of Different Coagulants in a Drinking Water Treatment Plant. International Journal of Advanced Science and Technology, 29**,** 8547-8555.

Zhang, S. & Shan, X.-Q. J. E. P. 2001. Speciation of rare earth elements in soil and accumulation by wheat with rare earth fertilizer application. Environmental Pollution, 112**,** 395-405.

Zhao, F., Cong, Z., Sun, H. & Ren, D. 2007. The geochemistry of rare earth elements (REE) in acid mine drainage from the Sitai coal mine, Shanxi Province, North China. International Journal of Coal Geology, 70**,** 184-192.

Zhao, Q., Liu, C., Shi, P., Zhang, B., Jiang, M., Zhang, Q., Saxén, H. & Zevenhoven, R. J. I. J. O. M. P. 2014. Sulfuric acid leaching of South African chromite. Part 1: Study on leaching behavior. 130**,** 95-101.

Zhu, G., Wu, X., Ge, J., Liu, F., Zhao, W. & Wu, C. 2020. Influence of mining activities on groundwater hydrochemistry and heavy metal migration using a self-organizing map (SOM). Journal of Cleaner Production, 257**,** 120664.

Zhu, M., Li, B. & Liu, G. 2022. Groundwater risk assessment of abandoned mines based on pressure-state-response—The example of an abandoned mine in southwest China. Energy Reports, 8**,** 10728-10740.

Ziemkiewicz, P., Noble, A. & Chris, V. 2021. Systems and processes for recovery of high-grade rare earth concentrate from acid mine drainage. Google Patents.